NeuroImage 247 (2022) 118746

Contents lists available at ScienceDirect

NeuroImage

journal homepage: www.elsevier.com/locate/neuroimage

# Ongoing neural oscillations influence behavior and sensory representations by suppressing neuronal excitability

Luca Iemi[a,b,*], Laura Gwilliams[c], Jason Samaha[d], Ryszard Auksztulewicz[e,f], Yael M Cycowicz[a,b], Jean-Remi King[g], Vadim V Nikulin[h,i], Thomas Thesen[j], Werner Doyle[j], Orrin Devinsky[j], Charles E Schroeder[a,k,l], Lucia Melloni[e,j], Saskia Haegens[a,b,m]

[a] Department of Psychiatry, Columbia University, College of Physicians and Surgeons, New York, NY, United States of America
[b] New York State Psychiatric Institute, New York, NY, United States of America
[c] Department of Neurological Surgery, University of California, San Francisco, CA, United States of America
[d] Department of Psychology, University of California, Santa Cruz, Santa Cruz, United States of America
[e] Department of Neuroscience, Max Planck Institute for Empirical Aesthetics, Frankfurt am Main, Germany
[f] Department of Neuroscience, City University of Hong Kong, Hong Kong, China
[g] Laboratoire des Systèmes Perceptifs, Département d'Études Cognitives, École Normale Supérieure, PSL University, CNRS, Paris, France
[h] Department of Neurology, Max Planck Institute for Human Cognitive and Brain Sciences, Leipzig, Germany
[i] Center for Cognition and Decision Making, Institute for Cognitive Neuroscience, National Research University Higher School of Economics, Moscow, Russian Federation
[j] Department of Neurology, New York University Langone Medical Center, New York City, United States of America
[k] Department of Neurological Surgery, Columbia University College of Physicians and Surgeons, New York, NY, United States of America
[l] Translational Neuroscience Division of the Center for Biomedical Imaging and Neuromodulation, Nathan Kline Institute, Orangeburg, NY, United States of America
[m] Donders Institute for Brain, Cognition and Behaviour, Centre for Cognitive Neuroimaging, Radboud University Nijmegen, Nijmegen, Netherlands

ARTICLE INFO

*Keywords:*
Alpha
Prestimulus
Oscillations
Excitability
Reaction times
Decoding

ABSTRACT

The ability to process and respond to external input is critical for adaptive behavior. Why, then, do neural and behavioral responses vary across repeated presentations of the same sensory input? Ongoing fluctuations of neuronal excitability are currently hypothesized to underlie the trial-by-trial variability in sensory processing. To test this, we capitalized on intracranial electrophysiology in neurosurgical patients performing an auditory discrimination task with visual cues: specifically, we examined the interaction between prestimulus alpha oscillations, excitability, task performance, and decoded neural stimulus representations. We found that strong prestimulus oscillations in the alpha+ band (i.e., alpha and neighboring frequencies), rather than the aperiodic signal, correlated with a low excitability state, indexed by reduced broadband high-frequency activity. This state was related to slower reaction times and reduced neural stimulus encoding strength. We propose that the alpha+ rhythm modulates excitability, thereby resulting in variability in behavior and sensory representations despite identical input.

## 1. Introduction

When asked to make repeated perceptual decisions, we often respond differently with each repetition, even when given the same sensory information (Rahnev and Denison, 2018; Wyart and Koechlin, 2016). We addressed the physiological sources of this variability by testing how ongoing fluctuations in alpha oscillations (7–14 Hz), thought to reflect neuronal excitability, affect behavior and neural sensory representations.

While historically regarded as "noise", ongoing neural oscillations strongly predict neural dynamics and behavior in health (Busch et al., 2009; Grabot and Kayser, 2020; Lange et al., 2013; Romei et al., 2008b; Samaha et al., 2020) and disease (age-related cognitive decline: Tran et al., 2020; Voytek et al., 2015; schizophrenia: Uhlhaas and Singer, 2010; autism: Simon and Wallace, 2016). Here, ongoing oscillations are operationalized as neural activity occurring without or preceding sensory stimulation (i.e., "prestimulus"); fluctuations in this activity are thought to be generated by both endogenous (e.g., arousal, motivation, top-down attention) and exogenous factors (e.g., behavioral paradigm, bottom-up attention). Numerous studies have shown that strong ongoing alpha oscillations are related to a state of low excitability, as indexed by a reduction of neuronal firing (Bollimunta et al., 2008, 2011; Chapeton et al., 2019; Dougherty et al., 2017; Haegens et al., 2011; Lundqvist et al., 2020; van Kerkoerle et al., 2014; Watson et al., 2018), local field potentials (Potes et al., 2014; Spaak et al., 2012), and hemodynamic activity (Becker et al., 2011; Goldman et al., 2002; Mayhew et al., 2013). Further, states of strong prestimulus alpha oscillations predict behavioral changes, including longer reaction

* Corresponding author.
*E-mail address:* luca.iemi@gmail.com (L. Iemi).

https://doi.org/10.1016/j.neuroimage.2021.118746.
Received 9 July 2021; Received in revised form 21 October 2021; Accepted 19 November 2021
Available online 4 December 2021.
1053-8119/© 2021 The Authors. Published by Elsevier Inc. This is an open access article under the CC BY-NC-ND license (http://creativecommons.org/licenses/by-nc-nd/4.0/)

times (RTs; Zhang et al., 2008; Bollimunta et al., 2008; Kelly and O'Connell, 2013; Bompas et al., 2015), lower probability of reporting near-threshold sensory stimuli (Ergenoglu et al., 2004; van Dijk et al., 2008; Busch et al., 2009; Mathewson et al., 2009; Chaumon and Busch, 2014; Iemi and Busch, 2018; Limbach and Corballis, 2016; Iemi et al., 2017; Craddock et al., 2017) or phosphenes (Romei et al., 2008a; Samaha et al., 2017), and reduced subjective perception (i.e., lower confidence: Samaha et al., 2017, 2020; lower visibility ratings: Benwell et al., 2017).

Despite this extensive work on alpha oscillations, the mechanisms supporting their apparent interrelation to excitability and behavior remain unclear. One proposal suggests that alpha oscillations reflect a mechanism of functional inhibition, regulating the excitability state of the neural system and thereby information processing necessary for behavior (Griffiths et al., 2019; Jensen and Mazaheri, 2010; Klimesch et al., 2007; Mathewson et al., 2011; Samaha et al., 2020; Stephani et al., 2020). At the physiological level, a state of functional inhibition may be achieved, for example, via the activation of GABAergic inhibitory interneurons and/or via reduced excitatory drive (e.g., downregulation of norepinephrine or acetylcholine). According to this account, the behavioral changes associated with alpha oscillations are caused by alpha power influencing neuronal excitability. Alternatively, alpha power might affect excitability and behavior via independent mechanisms (e.g., Gundlach et al., 2020). As most studies to date report evidence for a link between alpha power and either excitability or behavior, it is currently unknown whether the relationship between alpha power and behavior is mediated by a direct excitability modulation or via an independent mechanism.

It also remains unknown whether and how the excitability modulation associated with prestimulus alpha oscillations shapes the neural representations of sensory stimuli, on which behavior depends. Using decoding as a proxy for neural representation, we compared two hypotheses of how alpha oscillations may affect how sensory information is represented in the brain. First, low excitability during strong alpha oscillations may relate to a state of reduced attentional resources (Diepen and Mazaheri, 2017; Van Diepen et al., 2019), associated with decreased neural responses (Mehrpour et al., 2020; Treue and Maunsell, 1996) but increased variability/noise (Cohen and Maunsell, 2009; Mitchell et al., 2009). The resulting lower signal-to-noise ratio may thus worsen the encoding of sensory stimuli (i.e., lower decoder accuracy). Second, low excitability during strong alpha oscillations may be related to a decrease in the neural response magnitude and variability/noise (Goris et al., 2014; Tomko and Crapper, 1974). The resulting decrease in both signal and noise may thus reduce the overall strength of neural representations (i.e., lower decoder confidence; see Methods), leaving their encoding accuracy unaffected (Samaha et al., 2020).

Here, we tested the functional inhibition account of alpha oscillations and their effect on behavior and neural sensory representations by analyzing intracranial electroencephalography (iEEG) recordings in nine patients with medication-resistant epilepsy ($N$ = 1044 electrodes) while they categorized auditory stimuli (/PA/ or /GA/) preceded by different visual predictability cues (Fig. 1A; Auksztulewicz et al., 2018). Patients' task performance was at ceiling in terms of accuracy, but there was considerable variability in their reaction times, which allowed us to study how behavior changed from trial to trial. iEEG enabled us to estimate ongoing neural oscillations and broadband high-frequency activity (BHA, 70–150 Hz), which is thought to reflect neuronal ensemble activation patterns, including multiunit activity (Manning et al., 2009; Nir et al., 2007; Ray et al., 2008; Rich and Wallis, 2017; Ray and Maunsell, 2011; Miller et al., 2014), dendritic processes integral to excitation of neuronal ensembles (Leszczyński et al., 2020; Suzuki and Larkum, 2017), as well as additional neuronal processes such as synaptic currents (Lachaux et al., 2012). Critical for the present study, BHA provides a reliable measure of local neuronal excitability. First, we confirmed a hallmark of the functional inhibition account: i.e., a simultaneous negative relationship between ongoing alpha power and neuronal excitability (as indexed by BHA: Potes et al., 2014; Spaak et al., 2012). We tested whether this pattern generalizes across brain areas, whether it reflects a genuine oscillatory modulation, or a change in the aperiodic 1/f activity, and whether it is under top-down modulation by the predictability cues. Second, we tested whether prestimulus alpha power modulates the neural response to sensory stimuli (as indexed by poststimulus BHA), and whether this modulation generalizes across sensory modalities (i.e., visual and auditory). Third, we tested whether the effect of prestimulus alpha power on poststimulus excitability has consequences for task performance and for decoded neural stimulus representations. Specifically, we analyzed how prestimulus alpha power influences subsequent RTs, and we used mediation analysis to directly link prestimulus alpha power with RT changes via poststimulus excitability modulation. In addition, we used multivariate pattern analysis to test whether prestimulus alpha power affects decoder accuracy and/or confidence.

To preview our results, strong prestimulus oscillations in the alpha+ band (i.e., alpha and neighboring frequencies), rather than the aperiodic signal, are correlated with lower BHA, reflecting reduced excitability. This effect is observed across the brain and sensory modalities as well as before and after sensory input. Further, strong prestimulus alpha oscillations are correlated with slower RTs, and with a decrease in decoder confidence, but not accuracy. Critically, low excitability during the poststimulus window mediates the relationship between prestimulus alpha power and RTs, demonstrating a link between alpha oscillations, behavior, and excitability consistent with functional inhibition. We propose that, by modulating neuronal excitability, the ongoing alpha+ rhythm affects behavior and the strength of neural stimulus representations.

## 2. Results

### 2.1. Prestimulus alpha power negatively correlates with BHA

Based on the functional inhibition account of alpha oscillations, we hypothesized that a state of low neuronal excitability (here indexed by reduced BHA) would occur specifically during strong prestimulus alpha oscillations. An important aspect of the functional inhibition account is that it is specific to alpha-band oscillatory activity, rather than the aperiodic 1/f signal in the same frequency range. To address this, we sorted the recording sites into "periodic" and "aperiodic" based on the presence or absence of a (local) peak within the alpha frequency range of the prestimulus power spectrum in noise-locked epochs, respectively (following the methods in Haegens et al., 2014). Note that "prestimulus" in noise-locked epochs refers to the window before the onset of the noise image. To improve the spectral estimates, peak detection was based on trial-averaged data; we interpreted the peak in periodic sites as reflecting clear oscillatory (periodic) activity across trials, whereas the absence of a peak in aperiodic sites as indicating a more prominent 1/f aperiodic signal across trials (though, peaks may be present in individual trials, see Discussion). We found 525 periodic sites with alpha-band oscillatory activity (mean peak at 9 Hz, SEM=0.10), and 519 aperiodic sites with non-oscillatory 1/f activity in the alpha frequency range (Fig. 1B–D). Of note, periodic sites comprised 52% of the sites in the frontal lobe, 56% of the sites in the occipital lobe, 65% of the sites in the parietal lobe and 36% of the sites in the temporal lobe (see Fig. 1 supplement for more information on the topographical differences between periodic and aperiodic sites). We hypothesized a negative correlation between prestimulus BHA and alpha power specifically for periodic sites (where alpha-band power reflects a combination of oscillatory and aperiodic activity), but not in aperiodic sites (where alpha-band power reflects aperiodic activity).

To test this hypothesis, we sorted the power spectrum of the 1-s prestimulus window in noise-locked epochs into five bins based on single-trial estimates of alpha power (i.e., 7–14 Hz average) and computed the average BHA estimated in the same prestimulus window for each bin. This analysis focused on the prestimulus window as fluctuations

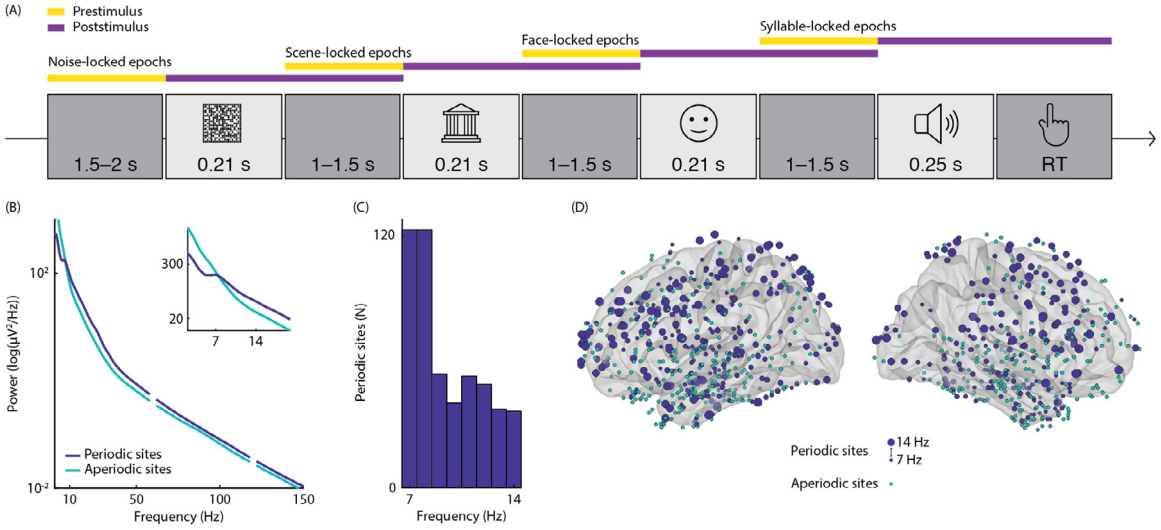


**Fig. 1.** Experimental paradigm and alpha-band periodic and aperiodic activity.
**A**. Schematic overview of the experimental paradigm. In each trial, participants were presented with a sequence of sensory stimuli in a fixed order: a noise image, a scene image, a face image, and a target syllable. At the end of the trial, participants reported the syllable identity (/ga/ or /pa/) via button press. Prestimulus and poststimulus windows are highlighted in yellow and purple, respectively, for each epoch type. **B.** Averaged power spectrum of the 1-s window before the noise image, shown separately for sites with alpha oscillations (periodic sites, in blue) and sites without a detectable alpha-band peak (aperiodic sites, in green). The inset shows the power spectrum for the frequency window of interest. **C.** Histogram of the alpha-band peak frequencies of the prestimulus power spectrum across periodic sites. **D**. Schematic illustration of the iEEG electrode coverage. Direct recordings of brain activity were obtained using intracranial electrodes implanted in 1044 sites across 9 epilepsy patients. Blue and green dots illustrate periodic and aperiodic sites, respectively; the size of blue dots indicates the alpha-band peak frequencies of periodic sites.

of spectral power during this window are assumed to be ongoing or endogenously generated. We used a repeated-measures mixed-effects ANOVA with BHA as dependent variable, periodic/aperiodic sites as between-unit factor (with units referring to recording sites), and alpha bins as within-unit factor. We found a significant main effect of alpha bins ($F(2.18, 2274.72)=64.72$, $p<0.001$; all ANOVAs Huynh-Feldt corrected) indicating that, across sites, BHA decreased with alpha power (bin 5 vs. bin 1: $t=-13.99$, $p<0.001$; all post-hoc comparisons Holm-Bonferroni corrected). Further, we found a significant main effect of periodic/aperiodic sites ($F(1, 1042)=71.50$, $p<0.001$), with higher BHA in periodic sites ($t = 8.46$, $p<0.001$). Critically, we found a significant interaction effect between periodic/aperiodic sites and alpha bins ($F(2.18, 2274.72)=53.73$, $p<0.001$), indicating that prestimulus BHA decreased with prestimulus alpha power in periodic sites (bin 5 vs. bin 1: $t=-19.51$, $p<0.001$; Fig. 2A/C/E), but not in aperiodic sites (bin 5 vs. bin 1: $t=-0.33$, $p = 1$; Fig. 2B/D), consistent with the functional inhibition hypothesis. An anatomical map of this effect in periodic sites (Fig. 2E) revealed a widespread BHA reduction during states of strong prestimulus alpha power across the brain.

We replicated the interaction effect using frequency-normalized BHA estimates ($F(2.21,2302.49)=50.50$, $p<0.001$; bin5 vs. bin1 in periodic sites: $t=-18.47$, $p<0.001$; bin5 vs. bin1 in aperiodic sites: $t = 0.42$, $p = 1$), confirming that prestimulus alpha power suppressed BHA after controlling for the 1/f contribution to BHA estimates.

Additionally, we replicated the interaction effect using four alternative methods for sorting the recording sites into periodic and periodic sites (see Methods), including peak detection using linear regression ($F(2.18, 2272.95)= 51.678$, $p<0.001$; bin5 vs. bin1 in periodic sites: $t=-19.44$, $p<0.001$; in aperiodic sites: $t=-0.08$, $p = 1$), gaussian fit ($F(2.17, 2258.16)= 44.27$, $p<0.001$; bin5 vs. bin1 in periodic sites: $t=-18.56$, $p<0.001$; in aperiodic sites: $t=-2.17$, $p = 0.28$), FOOOF ($F(2.08, 2078.19)= 6.982$, $p<0.001$; bin5 vs. bin1 in periodic sites: $t=-13.52$, $p<0.001$; in aperiodic sites: $t=-3.32$, $p = 0.010$), and eBOSC ($F(1.99,1385.40)= 19.94$, $p<0.001$; bin5 vs. bin1 in periodic sites: $t=-15.09$, $p<0.001$; in aperiodic sites: $t=-4.16$, $p = 0.001$).

We further corroborated these results by using a reversed approach: namely, we sorted epochs based on BHA magnitude (rather than alpha power) and analyzed the difference in low-frequency power across BHA bins (see Fig. 2 supplement for more detail). This approach revealed that BHA was negatively related to a range of low frequencies (4–40 Hz) including alpha and neighboring bands (i.e., alpha+), suggesting that functional inhibition is not exclusive to a narrow-band alpha rhythm.

Given that several previous studies observed that ongoing alpha power increases over the course of an experiment, possibly due to increasing fatigue (Benwell et al., 2017, 2018, 2019; Mathewson et al., 2009; van Dijk et al., 2008), it is important to rule out that the relationship between alpha power and excitability is confounded by changes in fatigue. First, we tested whether prestimulus alpha power in noise-locked trials was related to trial number (i.e., an indirect index of fatigue) using GLM: we found a significant positive correlation in periodic sites ($t(524)= 3.54$, $p<0.001$), consistent with previous studies (e.g., Benwell et al., 2019), and a significant negative relationship in aperiodic sites ($t(518)= -4.87$, $p<0.001$), possibly reflecting a flattening of the power spectrum (reduced alpha; Voytek et al., 2015) as a function of trial number. Then, we used GLM to estimate the relationship between prestimulus alpha power and BHA in noise-locked epochs while accounting for trial number: we found a significant negative correlation in periodic sites ($t(524)=-9.75$, $p<0.001$) and a significant positive relationship in aperiodic sites ($t(518)=6.62$, $p<0.001$), even after controlling for trial number (periodic sites: $t(524)=-6.42$, $p<0.001$; aperiodic sites: $t(518)= 5.31$, $p<0.001$), suggesting the relationship between power and excitability was not confounded by changes in fatigue.

In sum, these results suggest that reduced BHA is related to states of strong alpha oscillations, but not the aperiodic signal in the same frequency range, consistent with functional inhibition.

### 2.2. *Prestimulus alpha power and BHA are modulated by predictability cues*

In this study, patients were instructed to categorize auditory stimuli (/PA/ or /GA/) preceded by different visual predictability cues: temporal predictability was manipulated using regular or random intervals between the visual cues and the target syllable (i.e., in temporally-predictable blocks patients could predict target onset) whereas content

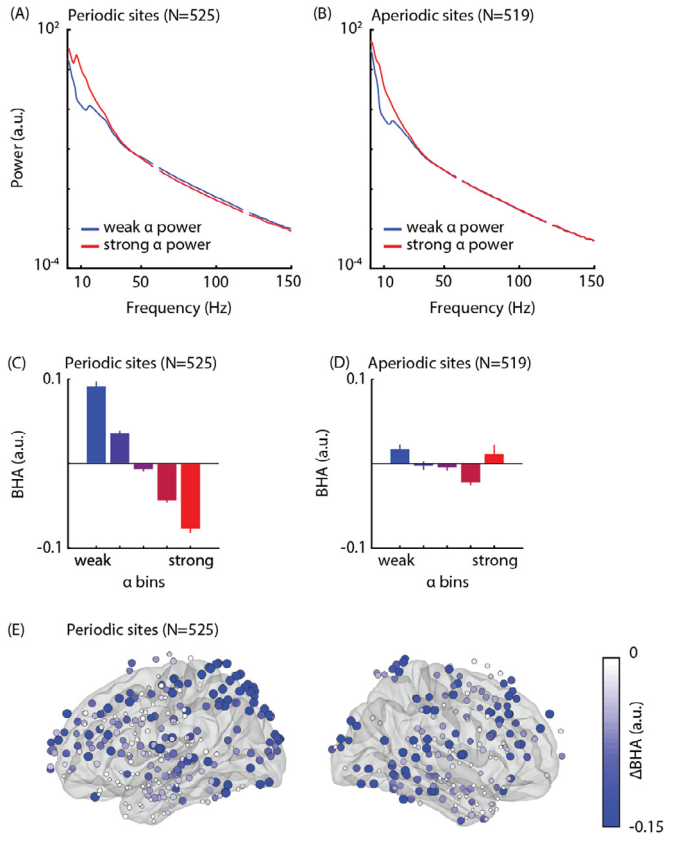


**Fig. 2.** Correlation between prestimulus alpha power and BHA.
**A.** Averaged power spectrum computed during the 1-s prestimulus window in noise-locked epochs, shown separately for bins of strongest (red) and weakest (blue) prestimulus alpha power for periodic sites (spectra normalized with average power). **B.** Same as A for aperiodic sites. **C.** Averaged BHA computed during the 1-s prestimulus window in noise-locked epochs (70–150 Hz) separately for five bins sorted from weakest (blue) to strongest (red) prestimulus alpha power (normalized with the average across bins) for periodic sites. BHA decreases with increased alpha power in periodic sites. **D.** Same as C for aperiodic sites. BHA is unaffected by the aperiodic signal in the alpha frequency range. **E.** Anatomical map of the relationship between prestimulus alpha power and BHA power in periodic sites, estimated as the normalized difference in BHA between bins of strongest and weakest alpha power. The color and size of the dots are proportional to the magnitude of this difference. The map shows negative effects (BHA in bin 5 < BHA in bin 1); no significant positive effects were found.

predictability was manipulated using contingencies between the visual cues and the target syllable (i.e., in content-predictable blocks patients could predict target identity based on specific visual cues). These predictability cues were manipulated blockwise, resulting in four conditions. Following the functional inhibition account, we hypothesized that visual cues resulting in temporal and content predictions lead to decreased alpha power and increased BHA during the prestimulus window in syllable-locked epochs, indicating increased excitability in anticipation of the task-relevant target stimuli.

To test this hypothesis, we estimated prestimulus alpha power and BHA in syllable-locked epochs separately for each predictability condition and site, and then used 2 × 2 repeated-measures mixed-effect ANOVAs with alpha or BHA as dependent variables, periodic/aperiodic sites as the between-unit factor, and temporal and content predictability conditions as within-unit factors. Note that "prestimulus" in syllable-locked epochs refers to the window immediately prior to syllable onset.

We found a significant main effect of temporal predictability on prestimulus alpha power ($F(1929)=99.460$, $p<0.001$), indicating that prestimulus alpha power was weaker in blocks when the stimulus onset was predictable compared to blocks when it was not (temporally predictable vs. unpredictable: $t=-9.973$, $p<0.001$). We found a significant main effect of content predictability on prestimulus alpha power ($F(1929)=12.684$, $p<0.001$), indicating that prestimulus alpha power was weaker in blocks when the stimulus identity was predictable compared to blocks when it was not (content-predictable vs. unpredictable: $t=-3.562$, $p<0.001$). There was a significant interaction effect between temporal and content predictability on prestimulus alpha power ($F(1929)=8.147$, $p = 0.004$), indicating that prestimulus alpha power was weaker in blocks with both predictable stimulus identity and onset (temporally and content-predictable vs. temporally and content- unpredictable: $t=-9.912$; $p<0.001$) compared to blocks with only predictable stimulus identity (temporally and content-predictable vs. temporally unpredictable and content-predictable: $t=-4.520$; $p<0.001$) or blocks with only predictable stimulus onset (temporally and content-predictable vs. temporally predictable and content-unpredictable: $t=-9.324$; $p<0.001$). Critically, there was a significant interaction between periodic/aperiodic sites and predictability, indicating that the difference in prestimulus alpha power between predictable and unpredictable conditions was bigger in periodic sites (temporal predictability: $F(1929) =27.28$, $p<0.001$; temporally predictable vs. unpredictable: $t=-10.648$; $p<0.001$; content predictability $F(1929) =14.64$, $p<0.001$; content-predictable vs. unpredictable: $t=-5.177$; $p<0.001$) compared to aperiodic sites (temporally predictable vs. unpredictable: $t=-3.390$, $p<0.001$; content-predictable vs. unpredictable: $t = 0.189$, $p = 0.850$).

In addition to prestimulus alpha power, we analyzed how predictability cues influence prestimulus BHA. We found a significant main effect of content predictability on prestimulus BHA ($F(1929)=19.031$, $p<0.001$), indicating that prestimulus BHA was stronger in blocks when the stimulus identity was predictable compared to blocks when it was not ($F(1929)=19.03$, $p<0.001$: content-predictable vs. unpredictable: $t = 4.362$, $p<0.001$). There was a non-significant trend for temporal predictability ($F(1929)=2.868$, $p = 0.091$; temporally predictable vs. unpredictable: $t = 1.693$, $p = 0.091$). Moreover, there was no significant effect of the interaction between content and temporal predictability ($F(1929)=0.003$, $p = 0.958$) and of the interaction between periodic/aperiodic sites and predictability (temporal predictability: $F(1929)=1.60$, $p<0.206$; content predictability: $F(1929) =1.676$, $p<0.196$).

In addition to alpha power and BHA, we analyzed how accuracy and reaction times were influenced by predictability using separate 2 × 2 repeated-measures factorial ANOVAs. We found an effect of predictability on neither accuracy (temporal predictability: $F(1)=0.585$, $p = 0.469$; content predictability: $F(1)=0.141$, $p = 0.718$; interaction: $F(1)=1.815$, $p = 0.220$) nor RT (temporal predictability: $F(1)=2.078$, $p = 0.193$; content predictability: $F(1)= 0.104$, $p = 0.757$; interaction: $F(1)=1.133$; $p = 0.323$), suggesting that these block-wise manipulations did not affect behavioral performance.

To summarize, these results indicate that (content) predictions are associated with a decrease of prestimulus alpha power specifically in periodic sites, and an increase in prestimulus BHA (before syllable onset), reflecting a state of increased excitability before the task-relevant stimulus. This pattern of results reflects a top-down modulation of alpha power and BHA, further supporting the functional inhibition account.

### 2.3. *Prestimulus alpha power negatively correlates with poststimulus BHA*

Based on the functional inhibition account, we hypothesized that, by setting the state of neuronal excitability, prestimulus alpha oscillations affect the processing of incoming stimulus information. To test this hypothesis, we sorted epochs into five bins based on prestimulus alpha power and computed the BHA during sensory processing: i.e., in the 1-s poststimulus window ("poststimulus" in noise-locked epochs refers to the window after the onset of the noise image). Note that, while prestimulus BHA reflects a measure of ongoing or "back-

ground" excitability, poststimulus BHA additionally includes event-related, stimulus-induced activity, reflecting the excitation to external stimulation. In noise-locked epochs, we found a significant main effect of alpha bin ($F(3.50, 3641.44)=24.87$, $p<0.001$), indicating that, across sites, poststimulus BHA (bin 5 vs. bin 1: $t=-9.27$, $p<0.001$) decreased with prestimulus alpha power (i.e., before noise image onset). Furthermore, we found a significant main effect of periodic/aperiodic sites ($F(1, 1042)=67.67$, $p<0.001$), with higher poststimulus BHA in periodic sites ($t = 8.23$, $p<0.001$). Critically, we found a significant interaction effect between periodic/aperiodic sites and prestimulus alpha bins ($F(3.562, 3711.934)=13.38$, $p<0.001$), indicating that, in periodic sites, BHA during the processing of the noise image decreased with alpha power estimated during the window preceding the noise image (bin 5 vs. bin 1: $t=-11.48$, $p<0.001$; Fig. 3A). By contrast, in aperiodic sites, poststimulus BHA was unrelated to prestimulus alpha power (bin 5 vs. bin 1: $t=-1.66$, $p = 0.880$). We obtained independent evidence for this effect when analyzing syllable-locked epochs. Note that "prestimulus" and "poststimulus" in syllable-locked epochs refer to the window before and after the onset of the syllable, respectively. Specifically, we found a significant interaction effect between periodic/aperiodic sites and prestimulus alpha bins on poststimulus BHA ($F(3.56, 3711.93)=13.38$, $p<0.001$, bin 5 vs. bin 1 in periodic sites: $t=-5.15$, $p<0.001$; Fig. 3B; in aperiodic sites: $t=-0.89$, $p = 1$) in syllable-locked epochs, suggesting that this effect generalizes across visual and auditory sensory stimulation.

We also compared BHA time-series between bins of strongest and weakest prestimulus alpha power separately for three regions of interest (ROI) based on functional and anatomical localizers. In the visual ROI ($N = 37$; Fig. 3G), we found two significant negative clusters, indicating that states of weak prestimulus alpha power coincided with weaker prestimulus BHA ($t=-116.59$, $p<0.001$; from −1 to 0.1 s) and were followed by weaker poststimulus BHA ($t=-24.52$, $p = 0.013$, from 0.35 to 0.6 s) in noise-locked epochs (Fig. 3H). These results were replicated during scene- (Fig. 3A supplement) and face-locked epochs (Fig. 3C supplement). Note that "prestimulus" and "poststimulus" in scene-locked (or face-locked) epochs refer to the window before and after the onset of the scene (or face) image, respectively. In the auditory ROI ($N = 55$; Fig. 3J), we found two significant negative clusters, indicating that states of weak prestimulus alpha power coincided with weaker prestimulus BHA ($t=-84.75$, $p<0.001$, from −1 to 0.1 s) and were followed by weaker poststimulus BHA ($t=-37.89$, $p<0.001$, from 0.3 to 0.85 s) in syllable-locked epochs (Fig. 3K). In the somatomotor ROI ($N = 64$; Fig. 3M), we found two significant clusters, indicating that states of weak prestimulus alpha power coincided with weaker prestimulus BHA ($t=-59.07$, $p = 0.002$; from −1 to −0.45 s) and were followed by weaker poststimulus BHA ($t=-46.61$, $p = 0.002$, from −0.3 to 0.25 s) in syllable-locked epochs (Fig. 3N). The ROI results suggest that this effect generalizes across visual, auditory and somatomotor areas.

Taken together, these results show that states of strong prestimulus alpha oscillations are followed by reduced poststimulus BHA across sensory modalities and brain areas, consistent with functional inhibition.

### 2.4. Prestimulus alpha power positively correlates with reaction times

Based on the functional inhibition account, we hypothesized that states of strong prestimulus alpha oscillations in task-relevant brain regions are followed by behavioral changes (e.g., slower RTs). To test this, we compared the RTs of the auditory discrimination task across states of weak and strong prestimulus alpha power in syllable-locked epochs.

We found a significant main effect of prestimulus alpha bins in syllable-locked epochs on RTs ($F(3.39, 3534.06)$ $t = 62.60$, $p<0.001$), indicating that RTs increased with prestimulus alpha power in both periodic (bin 5 vs. bin 1: $t = 11.94$, $p<0.001$; Fig. 3E) and aperiodic sites (bin 5 vs. bin 1: $t = 12.92$, $p<0.001$). The mean RT difference between states of strong and weak prestimulus alpha power in periodic sites was 0.011 s (SEM= 27) with a maximum of 0.235 s in the caudal division of the middle frontal gyrus, while in aperiodic sites it was 0.018 s (SEM= 23) with a maximum of 0.143 s in the postcentral gyrus. An anatomical map of the RT difference in periodic sites revealed that slow RTs were preceded by strong pre-syllable alpha power across the brain (Fig. 3F). In addition, we found a significant interaction effect ($F(3.39, 3534.06)=3.09$, $p = 0.021$), suggesting a trend for slower RTs in the strongest alpha bin in aperiodic sites (periodic vs. aperiodic sites for bin 5: $t=-2.95$, $p = 0.067$). Note that the effect of prestimulus alpha power on RTs was present during syllable-locked epochs in both auditory (bin 5 vs. bin 1: $t(54)=3.32$, $p = 0.002$) and somatomotor ROIs (bin 5 vs. bin 1: $t(63)=6.94$, $p<0.001$). By contrast, no significant effects were found in noise- (Fig. 3I), scene- (Fig. 3B supplement) and face-locked epochs (Fig. 3D supplement) in the visual ROI ($p>0.05$), indicating that auditory RTs were affected only by alpha power right before the target auditory stimulus.

In sum, these results demonstrate that states of strong prestimulus alpha oscillations—as well as the aperiodic signal in the same frequency range—are followed by slower RTs. However, it should be noted that this result alone does not constitute evidence for the functional inhibition account of alpha oscillations since it is not specific to oscillatory activity.

### 2.5. The correlation between prestimulus alpha power and RT is mediated by poststimulus BHA

There are two alternative accounts on the inter-relationship between alpha oscillations, excitability, and behavior: based on the functional inhibition account, we hypothesized that the RT effect associated with prestimulus alpha oscillations (rather than the aperiodic signal) was specifically mediated by a modulation of poststimulus BHA in syllable-locked epochs; alternatively, prestimulus alpha oscillations may affect BHA and behavior via independent mechanisms without mediation. To distinguish between these two accounts, we estimated the mediation effect by analyzing the trial-by-trial interrelation between alpha power, RTs, and BHA using a causal step approach based on GLM (Judd and Kenny, 1981; Fig. 4AC, see Methods). Specifically, this approach consists in analyzing the correlation coefficients of four GLMs separately for each site: a linear regression with prestimulus alpha power predicting poststimulus BHA; a linear regression with poststimulus BHA predicting RTs; a linear regression with prestimulus alpha power predicting RTs; and a multiple regression with both prestimulus alpha power and poststimulus BHA predicting RTs.

Confirming the results of the binning analysis (Fig. 3B), we found that prestimulus alpha was negatively correlated with poststimulus BHA in periodic sites ($t(524)=-3.569$, $p<0.001$; $a<0$ in Fig. 4A), consistent with functional inhibition, whereas it was positively correlated with poststimulus BHA in aperiodic sites ($t(518)=2.22$, $p = 0.027$) ($a>0$ in Fig. 4B), consistent with a change in the offset of the power spectrum (i.e., upward shift at all frequencies). In addition, we found that poststimulus BHA was negatively correlated with RTs across all sites (periodic: $t(524)=-2.03$, $p = 0.043$; aperiodic: $t(518)=-5.85$, $p<0.001$) ($b>0$ in Fig. 4B), even after controlling for prestimulus alpha power (periodic: $t(524)=-1.98$, $p = 0.048$; aperiodic: $t(518)=-5.92$, $p<0.001$) (b'<0 in Fig. 4B). Moreover, we found that prestimulus alpha was positively correlated with RTs in periodic ($T(524)=7.33$, $p<0.001$) and aperiodic sites ($T(518)=11.18$, $p<0.001$) (c in Fig. 4B), even after controlling for poststimulus BHA (periodic: $t(524)=6.77$, $p<0.001$; aperiodic: $t(518)=10.93$, $p<0.001$; c'>0 in Fig. 4B), suggesting partial mediation (see Methods).

To test for mediation, we estimated the indirect effect by computing the reduction in the effect of prestimulus alpha power on RTs after accounting for poststimulus BHA. We found a significant indirect effect in periodic sites ($t(524)=3.41$, $p<0.001$), supporting mediation, but not in aperiodic sites ($t(518)=0.26$, $p = 0.795$; c-c' in Fig. 4D). This effect was indeed larger in sites with periodic activity (unpaired $t(1042)=3.22$, $p = 0.001$). An anatomical map of the indirect effect in periodic sites re-

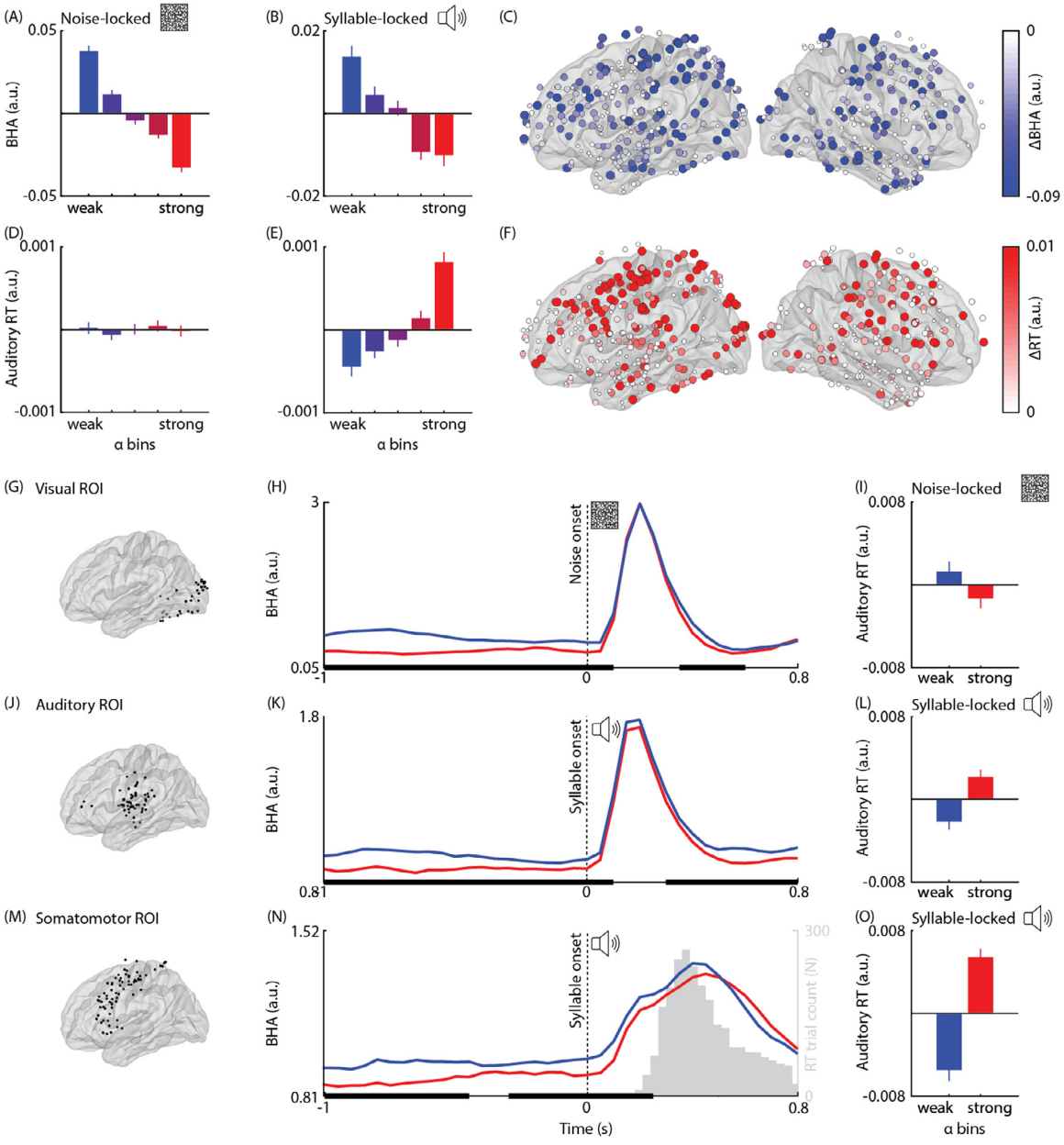


**Fig. 3.** Correlation between prestimulus alpha power, poststimulus BHA, and reaction times.
**A/B.** Averaged poststimulus BHA, shown separately for five bins sorted from weakest (blue) to strongest (red) prestimulus alpha power in periodic sites in noise-locked and syllable-locked epochs, respectively. In periodic sites, BHA after the onset of the noise image and the syllable decreases with prestimulus alpha power, consistent with functional inhibition. The error bars represent SEM across sites. **C.** Anatomical map of the relationship between prestimulus alpha power and poststimulus BHA in periodic sites, estimated as the normalized difference between bins of strongest and weakest alpha power. The color and size of the dots are proportional to the experimental effect. The map shows negative effects (BHA in bin 5 < BHA in bin 1) in noise-locked epochs. No significant positive effects were found. **D/E.** Same as in A/B for RT in noise- and syllable-locked epochs, respectively. RT increases with prestimulus alpha power in syllable-locked epochs, but not in noise-locked epochs. **F.** Same as in C for RT. The map shows positive effects (RT in bin 5 > RT in bin 1) in syllable-locked epochs. No significant negative effects were found. **G.** Anatomical map of the visual ROI, including periodic sites that were functionally and anatomically related to visual cues. **H.** BHA time-course shown separately for bins of weakest (blue) and strongest (red) prestimulus alpha power for noise-locked epochs in the visual ROI. Bold horizontal black lines indicate significant differences using cluster permutation testing. States of strong prestimulus alpha power are related to a BHA reduction during the prestimulus and poststimulus windows, consistent with functional inhibition. **I.** Averaged RT, shown separately for the weakest (blue) and strongest (red) bin of prestimulus alpha power in noise-locked epochs in the visual ROI. RT is affected by alpha power before the syllable in both auditory and somatomotor areas, but not before the noise image in visual areas. **J.** Same as G for the auditory ROI, including periodic sites that were functionally and anatomically related to target syllables. **K/L.** Same as H/I for syllable-locked epochs in the auditory ROI. **M.** Same as G for the somatomotor ROI, including periodic sites that were functionally and anatomically related to motor responses. **N/O.** Same as H/I for syllable-locked epochs in the somatomotor ROI.

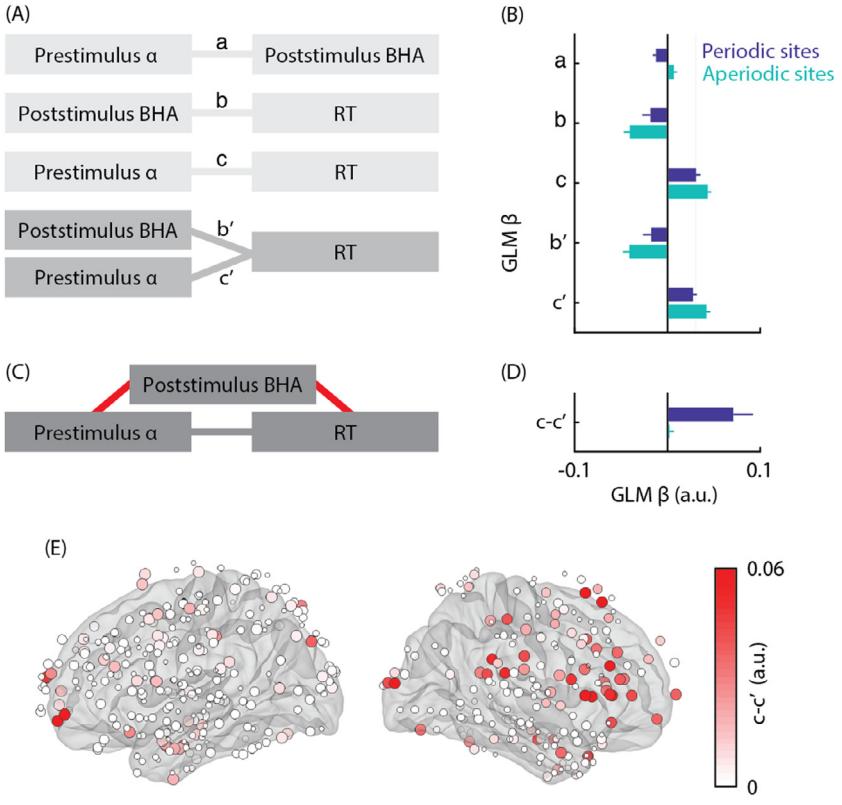


**Fig. 4.** Mediation between prestimulus alpha power, poststimulus BHA, and reaction time.
**A.** Schematic illustration of the causal path mediation analysis using four GLMs, characterizing the interrelation between prestimulus alpha oscillations (i.e., the independent variable), RTs (i.e., the dependent variable), and poststimulus BHA (i.e., the mediator) in syllable-locked epochs: a represents the relationship of independent variable to the mediator, b the mediator to dependent variable, c the independent variable to dependent variable, b' the mediator to dependent variable adjusted for independent variable, and c' the independent variable to dependent variable adjusted for mediator. The variables and the relationships among them are represented by rectangles and lines, respectively. **B.** Averaged effects of the causal path mediation analysis showing the interrelation between prestimulus alpha power, poststimulus BHA, and RTs, shown separately for periodic (blue) and aperiodic sites (green). These effects are estimated using the averaged zero-order (a–c) and partial GLM coefficients (b'/c') and their comparison (c-c') based on causal path mediation analysis in (A). The error bars represent SEM across sites. **C.** Theoretical mediation model in which the independent variable leads to the dependent variable via an indirect effect through the mediator (red path). **D.** Averaged indirect effect reflecting the mediation between prestimulus alpha power and RT via poststimulus BHA, shown separately for periodic (blue) and aperiodic sites (green). In periodic sites, the effect of prestimulus alpha power on RTs is significantly reduced after accounting for poststimulus BHA (c-c'>0), demonstrating an indirect effect, consistent with functional inhibition. In aperiodic sites, the relationship between prestimulus alpha power and RTs is unaffected by poststimulus BHA (c-c'=0), suggesting no indirect effect. **E.** Anatomical map of the magnitude of the indirect effect in periodic sites. The color and size of the dots are proportional to the experimental effect.

vealed this effect occurred across several sites with maxima in the pars triangularis and the rostral division of the middle frontal gyrus (Fig. 4E).

Together, these findings support the functional inhibition account by demonstrating that the modulation of poststimulus excitability mediates the behavioral effects of alpha oscillations, rather than the aperiodic signal in the same frequency range.

### 2.6. *Prestimulus alpha power negatively correlates with neural stimulus feature encoding*

Based on the functional inhibition account, we hypothesized that the effect of prestimulus alpha power on poststimulus neuronal excitability may affect how stimulus features are encoded in BHA estimates in syllable-locked epochs. Specifically, we tested whether prestimulus alpha power affects (1) decoding accuracy, which reflects sensory precision or (2) decoding confidence, which reflects the strength of sensory encoding. To test this, we used "spatial decoding" (Gwilliams and King, 2020): separately for each electrode, we predicted syllable identity (labels: /ga/ vs. /pa/) by fitting logistic regression decoders on the single-trial temporal BHA patterns as input (see Fig. 5B supplement for a comparison with the low-passed signal). First, decoder accuracy was estimated as the similarity between the probabilistic prediction (normalized distance from the hyperplane) and true labels using the area under the curve (AUC). Second, stimulus encoding strength or decoder confidence was estimated as the maximum probabilistic prediction, regardless of its accuracy (i.e., whether or not it matched the true label). Across sites there was a significant positive correlation between decoder accuracy and confidence averaged over trials (Spearman rho=0.15, $p<0.001$), demonstrating that sites which encode syllable identity more reliably also tend to exhibit higher confidence in those predictions. Moreover, to understand how these decoder metrics were related to the participant's behavior on a trial-by-trial basis, we correlated RTs with single-trial accuracy (binarized into correct and incorrect) and confidence of the decoder predictions using GLM for each site. Across sites there was a significant negative correlation between RTs and both decoder accuracy ($t(1043)=-2.75$, $p = 0.006$) and confidence ($t(1043)= -3.45$, $p<0.001$), indicating that higher decoder accuracy and confidence were related to faster RTs.

Next, we tested whether prestimulus oscillatory state influences decoded neural stimulus representations. For each site, we computed single-trial probabilistic estimates for each syllable based on BHA temporal patterns. Then, we sorted the trials based on the 1-s prestimulus alpha power (in syllable-locked epochs) and estimated decoder accuracy and confidence using these probabilistic estimates separately for each bin. We compared decoder accuracy (AUC) across alpha bins in periodic and aperiodic sites and found no significant effects ($p>0.05$; Fig. 5AB), suggesting that the precision of neural stimulus representation/encoding was unlikely affected by prestimulus alpha power. We also compared decoder confidence across alpha bins in periodic and aperiodic sites and found a significant interaction effect ($F(3.96, 4125.61)=2.59$, $p = 0.036$), such that stimulus encoding strength nominally decreased with alpha power in periodic sites (bin 5 vs. bin 1: $t =-1.89$, $p = 1$; Fig. 5C), while it nominally increased in aperiodic sites (bin 5 vs. bin 1: $t = 0.87$, $p = 1$; Fig. 5D), although these post-hoc effects were not significant after correcting for multiple comparisons. Additionally, this interaction effect was significant in trials with correct predictions ($F(4.00, 4166.49)=3.54$, $p = 0.007$) and trending toward significance in trials with incorrect predictions ($F(3.99, 4148.44)=2.06$, $p = 0.084$), suggesting that strong prestimulus alpha power in periodic sites decreased stimulus encoding strength (and vice versa in aperiodic sites) regardless of the accuracy of stimulus encoding. An anatomical map of the effect on confidence in periodic sites revealed a widespread reduction following states of strong prestimulus alpha power across the brain (Fig. 5E).

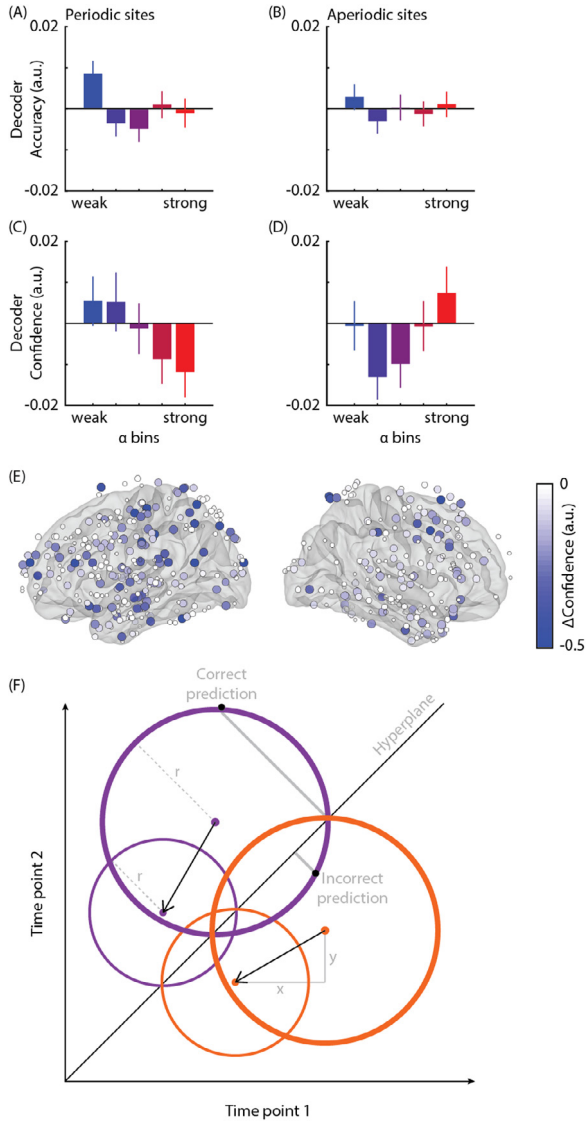


**Fig. 5.** Correlation between prestimulus alpha power and neural stimulus decoding.

**A**. Averaged normalized decoder accuracy (AUC) for decoding syllable identity from BHA shown separately for five bins sorted from weakest (blue) to strongest (red) prestimulus alpha power in periodic sites. The error bars represent SEM across sites. **B.** Same as A in aperiodic sites. Decoder accuracy is affected by prestimulus alpha power in neither periodic nor aperiodic sites. **C.** Same as A for decoder confidence. **D.** Same as C for aperiodic sites. Decoder confidence decreases with prestimulus alpha power in periodic sites whereas it increases in aperiodic sites. **E.** Anatomical map of the magnitude of the effect of the decoder confidence in periodic sites. The color and size of the dots are proportional to the experimental effect. The map shows negative effects (confidence in bin 5 < confidence in bin 1). No significant positive effects were found. **F.** Model of the relationship between alpha oscillations and decoding performance. In a two-dimensional activation space, each trial is characterized by the activity values estimated at two time points from a single electrode (i.e., activation point). Response distributions are shown by purple (for stimulus A) and orange circles (for stimulus B) with center and radius representing response mean and variability, respectively. Learning a linear classifier (A vs B) is equivalent to learning the hyperplane (diagonal line) that best separates the two distributions: if distance between an activation point and the hyperplane > 0, then the classifier predicts "A", otherwise "B". This model assumes that states of low excitability indexed by strong alpha oscillations are related to reduced distributions' mean (arrow), and variability, resulting in a decrease of the absolute distance of the activation points from the hyperplane (i.e., lower decoder confidence), while leaving the distributions' overlap (i.e., decoder accuracy) unaffected.

We also tested whether, in periodic sites, the effects of alpha power on decoder accuracy and confidence (i.e., bin 5 vs. bin 1) were dependent on two site-specific characteristics: the negative relationship between ongoing alpha power and BHA (i.e., index of functional inhibition), and overall decoder accuracy. We found no across-site correlation ($p$>0.05) between overall decoder accuracy and the effects of alpha power on decoder accuracy and confidence, or between the alpha-BHA relationship and the effect on decoder accuracy, indicating that decoder accuracy was unrelated to the confidence effect and to prestimulus power. By contrast, we found a significant positive across-site correlation between the alpha-BHA relationship and the effect of alpha power on decoder confidence (Spearman rho=0.103, $p$ = 0.019), suggesting that, during states of strong prestimulus alpha power, the stronger the inhibition associated with alpha power, the lower the decoder confidence. We corroborated this finding in sites with a negative alpha-BHA relationship, reflecting functional inhibition: we found a significant effect of alpha bins on decoder confidence (F(3.891, 1338.467)=3.69, $p$ = 0.006), indicating that decoder confidence decreased with prestimulus alpha power (bin 5 vs. bin 1: $t$ =−2.86, $p$ = 0.039).

It could be argued that, due to their relatively strong signal-to-noise ratio, states of strong alpha oscillations act as a source of noise (e.g., degrading the signal at other frequencies), resulting in lower decoder performance without affecting neural stimulus representations. To rule out this alternative account, we tested whether overall decoder accuracy and/or confidence were lower in periodic sites, which have stronger alpha power compared to aperiodic sites (Fig. 1 supplement). The results showed that periodic and aperiodic sites differed in neither accuracy (unpaired t(1042)=1.12, $p$ = 0.264) nor confidence (t(1042)= 0.750, $p$ = 0.453), suggesting that differences in alpha oscillatory activity between sites are unlikely to act as a noise source for decoder performance.

In sum, these findings extend the functional inhibition account by demonstrating that states of strong prestimulus alpha power reduce the strength, but not the precision, of neural stimulus representations.

### 2.7. *Baseline shift of alpha oscillations affects ERPs but not BHA*

Finally, we assessed if the observed relationship between alpha oscillations and BHA is determined by mechanisms other than functional inhibition (i.e., baseline shift of non-zero-mean oscillations) that affect event-related potentials (ERP; Nikulin et al., 2007; Mazaheri and Jensen, 2008; Iemi et al., 2019). Baseline shift predicts that the relationship between alpha power and neural signals depends on the direction of the baseline shift (which can also be viewed as polarity) of non-zero-mean oscillations (Fig. 6AB), whereas functional inhibition predicts a negative relationship between alpha power and neural signals (reflecting excitability) regardless of oscillatory polarity

To test for these mechanisms, we quantified the polarity of the baseline shift using the baseline shift index (BSI), which reflects the correlation between the alpha power envelope and the low-passed EEG signal in continuous data. A positive polarity (BSI > 0) indicates that strong alpha power is correlated with an increase of the low-passed signal, as expected for positive-mean oscillations, whereas a negative polarity (BSI < 0) indicates that strong alpha power is correlated with a decrease of the low-passed signal, as expected for negative-mean oscillations. We identified 323 sites with a negative oscillatory mean (Fig. 6CE) and 202 sites with a positive oscillatory mean (Fig. 6DF) using the baseline shift index (BSI), and analyzed how prestimulus oscillations with different polarities affect ERP and BHA in noise-locked epochs.

We found a significant interaction effect between polarity (i.e., sites with positive or negative mean) and prestimulus alpha bin on the prestimulus (F(1.79, 935.91)=120.45, $p$<0.001) and poststimulus ERP (F(1.67, 873.44)=139.55, $p$<0.001; Fig. 6GH). Compared to the weakest alpha bin, the prestimulus ERP baseline of the strongest alpha bin was characterized by a more negative voltage in sites with a negative mean (bin 5 vs. bin 1: $t$=−19.48, $p$<0.001), and more positive voltage in sites with a positive mean (bin 5 vs. bin 1: $t$ = 10.09, $p$<0.001). Fur-

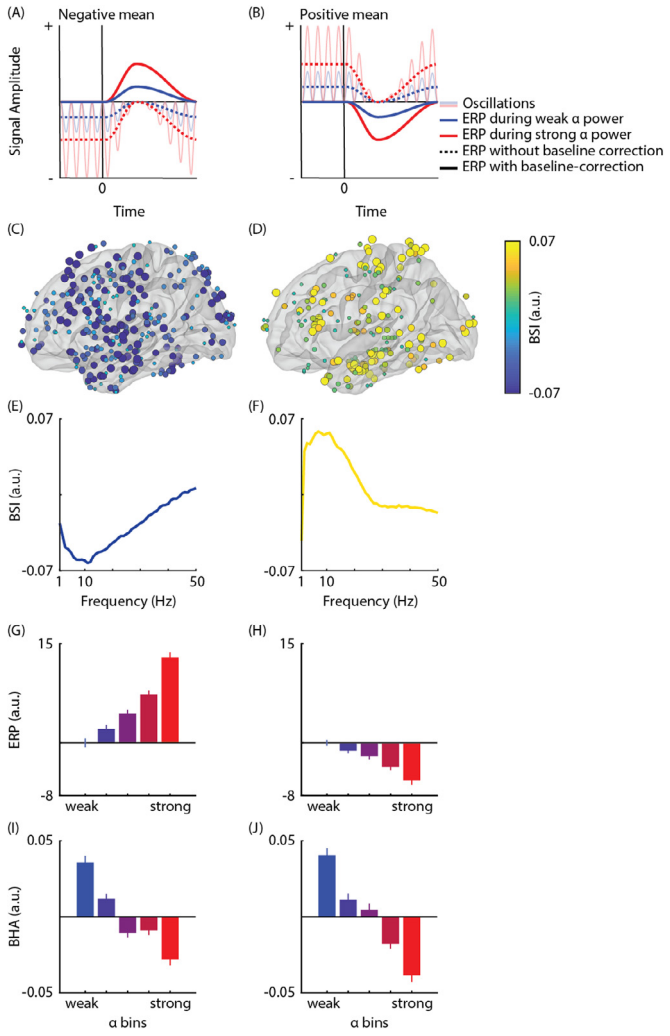


**Fig. 6.** Correlation between alpha power and BHA accounting for baseline shift of non-zero-mean oscillations

**A/B.** Neural oscillations are modelled as sinusoidal waveforms (opaque lines) varying asymmetrically around a non-zero mean. Unlike zero-mean oscillation, trial averaging of non-zero-mean oscillations does not eliminate non-phase-locked oscillations in the prestimulus window, resulting in an ERP prestimulus baseline with an offset (dotted lines). During event-related desynchronization (ERD) by stimulus onset (vertical line), the averaged signal gradually approaches the zero line of the signal. When the poststimulus signal is corrected with the prestimulus non-zero baseline, a slow shift of the ERP signal appears (thick lines), mirroring the ERD. The baseline-shift mechanism predicts that: (1) the polarity of the non-zero mean baseline determines the directionality of the effect of prestimulus oscillations on the ERP signal (in raw values); (2) the poststimulus ERP signal is amplified (in absolute values) during states of strong prestimulus alpha power. **C/D.** Anatomical map of the magnitude of the baseline-shift-index (BSI) averaged across the alpha band shown separately for periodic sites with negative- and positive-mean alpha oscillations, respectively. **E/F.** Magnitude of the baseline-shift-index (BSI) represented for frequencies between 1 and 50 Hz, separately for sites with negative- and positive-mean alpha oscillations, respectively. **G/H.** ERP magnitude averaged across the 1-s poststimulus window, shown separately for five bins sorted from weakest (blue) to strongest (red) prestimulus alpha power in periodic sites with negative and positive mean oscillations, respectively. The estimates were normalized, first, with the average across bins and, second, with the magnitude of the weakest bin, which is assumed to best reflect the zero line of the signal. The relationship between prestimulus alpha power and poststimulus ERP (in raw values) depends on the non-zero-mean property of alpha oscillations. States of strong prestimulus alpha power results in ERP amplification (in absolute values), consistent with baseline shift. The error bars represent SEM across sites. **I/J.** Averaged poststimulus BHA shown separately for five bins sorted from weakest (blue) to strongest (red) prestimulus alpha power in periodic sites with negative and positive mean oscillations, respectively (normalized with the average across bins). There is a negative relationship between prestimulus alpha power and poststimulus BHA regardless of the polarity of the oscillatory mean, consistent with functional inhibition.

thermore, compared to the weakest alpha bin, the ERP averaged over the poststimulus window of the strongest alpha bin was characterized by a more positive voltage shift in sites with a negative mean (bin 5 vs. bin 1: $t = 23.99$, $p<0.001$; Fig. 6G), and more negative voltage shift in sites with a positive mean (bin 5 vs. bin 1: $t=-8.39$, $p<0.001$; Fig. 6H). In other words, states of strong prestimulus alpha power are related to a stronger non-zero ERP baseline, which is followed by an ERP amplification in the poststimulus window, consistent with a baseline shift of non-zero-mean alpha oscillations.

By contrast, we found a significant main effect of prestimulus alpha bins on both prestimulus ($F(2.11, 1104.11)=99.79$, $p<0.001$) and poststimulus BHA ($F(3.51, 1834.91)=28.93$, $p<0.001$), indicating that BHA decreased with prestimulus alpha power in sites with both a negative (bin 5 vs. bin 1 for prestimulus BHA: $t=-12.78$, $p<0.001$; poststimulus BHA: $t=-7.85$, $p<0.001$; Fig. 6I), and positive mean (prestimulus BHA: $t=-12.86$, $p<0.001$; poststimulus BHA: $t=-6.40$, $p<0.001$; Fig. 6L), consistent with functional inhibition. Indeed, there was no significant interaction effect between polarity and prestimulus alpha bin on prestimulus or poststimulus BHA ($p>0.05$). In addition, we found a significant main effect of polarity on both prestimulus ($F(1, 523)=8.48$, $p = 0.004$) and poststimulus BHA ($F(1, 523)=7.30$,$p = 0.007$), indicating that sites with a negative oscillatory mean were characterized by overall greater BHA (prestimulus BHA: $t = 2.91$, $p = 0.004$; poststimulus BHA: $t = 2.70$, $p = 0.007$). We replicated these effects in a control analysis using the Amplitude Fluctuation Asymmetry Index (AFAI: Mazaheri and Jensen, 2008) to identify sites with a negative and positive asymmetries in oscillatory peaks (Fig. 6 supplement). In sum, these results demonstrate that the negative relationship between alpha power and BHA is consistent with functional inhibition, rather than baseline shift of non-zero mean alpha oscillations.

## 3. Discussion

### 3.1. Simultaneous relationship between alpha oscillations and excitability

We hypothesized that alpha oscillations reflect functional inhibition, regulating the excitability state of the neural system. To test this, we analyzed the relationship between alpha power and BHA which is considered a proxy for neuronal ensemble excitability. Though BHA is often referred to as “high gamma,” it is physiologically distinct from narrowband gamma oscillations reflecting rhythmic activity between 30 and 70 Hz. Initially thought to reflect net local neuronal firing—i.e., multiunit activity (Manning et al., 2009; Nir et al., 2007; Ray et al., 2008; Ray and Maunsell, 2011; Rich and Wallis, 2017; Whittingstall and Logothetis, 2009), it was shown more recently that BHA mainly indexes calcium-dependent dendritic processes that, albeit correlated with firing probability, are separable from it (Leszczyński et al., 2020). This suggests that in relative terms, BHA is a more direct measure of neuronal excitability. There is also indication that BHA signals may volume-conduct over greater distances than multiunit activity signals (Leszczyński et al., 2020), making BHA a more useful measure of neuronal ensemble excitability. Our findings confirmed the functional inhibition account by showing that states of strong ongoing oscillations in the alpha+ band (i.e., alpha and neighboring frequencies) were related to reduced BHA, indicating a state of low neuronal excitability.

These findings corroborate studies reporting that strong alpha oscillations are related to reduced neuronal firing in animal models (Haegens et al., 2011; Watson et al., 2018) and reduced fMRI BOLD signal in humans (Chapeton et al., 2019; Mayhew et al., 2013). Additionally, they are also consistent with numerous studies suggesting a negative relationship between low-frequency power, including the al-

pha band, and high-frequency power, including BHA, during sensory, motor and task processing. Specifically, increased high-frequency power co-occurred with decreased low-frequency power after the presentation of visual (Lachaux et al., 2005; Martin et al., 2019; Nir et al., 2007, 2017; Rodriguez et al., 2004; Fisch et al., 2009; Miller et al., 2014; Podvalny et al., 2015; Fries et al., 2001; Scheeringa et al., 2011; Hwang and Andersen, 2011; Rickert et al., 2005; Lundqvist et al., 2020; Haegens et al., 2021), auditory (de Pesters et al., 2016; Potes et al., 2014), and somatosensory stimuli (Fontolan et al., 2014), and during motor responses (Crone et al., 1998; de Pesters et al., 2016; Jiang et al., 2020; Miller et al., 2007) and task/cognitive processing (Hwang and Andersen, 2011). Several M/EEG studies observed a negative relationship between low-frequency power decrease and, what is reported as, narrowband gamma increase (Bauer et al., 2006; Kloosterman et al., 2019; van Ede et al., 2014; Wyart and Tallon-Baudry, 2009); though it remains unclear whether this high-frequency signal reflects genuine oscillatory activity or broadband power. Importantly, the negative relationship between low- and high-frequency power was recently linked to changes in cognitive function (Nir et al., 2007; Proskovec et al., 2019; Tran et al., 2020; Voytek et al., 2015).

In this study, rather than analyzing how BHA and alpha power change as a function of sensory/task processing, we systematically estimated the trial-by-trial correlation between these signals in intracranial human recordings. First, we analyzed a wide range of brain areas spanning from primary sensory cortices to frontal regions, by which we overcome some limitations in previous studies estimating neural signals in a limited set of brain areas. Our findings show a negative relationship between alpha power and BHA occurring across the whole brain, consistent with the idea that functional inhibition reflects a general property of alpha oscillations.

Second, some investigators have questioned whether the negative correlation between low- and high-frequency power reflects an oscillatory modulation driven by the alpha rhythm or whether it is due to a change of the aperiodic signal (McNair et al., 2019; Podvalny et al., 2015; Voytek et al., 2015). Note that the power spectrum contains not only oscillatory/periodic activity, but also an aperiodic signal (1/f background noise), parametrized by an offset and a slope (Donoghue et al., 2020). While an increase in the offset of the aperiodic signal may boost power at all frequencies, an increase in aperiodic slope may manifest as a simultaneous increase in low-frequency power and a decrease in high-frequency power. Critically, sorting trials by the power in a predefined frequency band (e.g., alpha) in different bins has been shown to affect both the slope and offset of the aperiodic signal (Iemi et al., 2019). Therefore, it is possible that the reduced BHA during states of strong alpha power can be explained by a steeper slope of the aperiodic signal. Moreover, the aperiodic signal is thought to reflect a physiological function (Voytek et al., 2015) that is, at least partially, independent from the periodic signal. Accordingly, distinguishing between an oscillatory or aperiodic modulation driving the alpha-BHA relationship is critical for understanding the underlying neural mechanisms. In periodic sites, containing both periodic/oscillatory and aperiodic activity, it is not possible to distinguish between the oscillatory and aperiodic modulations because we expect the same negative relationship between alpha power and BHA, regardless of the underlying modulation. By contrast, in aperiodic sites, we can make separate predictions for the oscillatory and aperiodic modulations. If, on the one hand, the alpha-BHA relationship reflects an aperiodic modulation (i.e., change of the aperiodic slope), then we expect a negative relationship in aperiodic sites: namely, states of strong aperiodic power in the alpha range may be related to a steeper aperiodic slope, resulting in lower BHA. If, on the other hand, the alpha-BHA relationship reflects an oscillatory modulation, then we expect a positive relationship in aperiodic sites: namely, states of strong aperiodic power in the alpha range may be related to a higher offset of the power spectrum (i.e., upward shift at all frequencies), resulting in higher BHA. Our results are consistent with an oscillatory modulation, showing a negative relationship between BHA and alpha power in periodic sites, and a positive relationship in aperiodic sites (see GLM results in Fig. 4B). It should be noted that the sorting into periodic and aperiodic sites may have suffered from some methodological limitations, which, however, did not substantially affect our conclusions. Note that the sorting was based on the peak detection in the trial-averaged prestimulus power spectrum because it provides a more accurate spectral estimate than that of individual trials, where, due to lower signal-to-noise ratio, it can be difficult to distinguish whether a peak reflects spurious or genuine oscillatory activity. Accordingly, the power spectrum of some trials in sites designated as aperiodic may actually contain genuine alpha-band periodic activity. Furthermore, some periodic sites may have been mislabeled as aperiodic, when, for example, due to the 1/f signal, peaks in delta and theta power conceal smaller peaks in the alpha range. To address this issue, we replicated the results using alternative peak detection methods which account for the 1/f signal (see Methods). Together, these limitations may increase the similarity between periodic and aperiodic sites—however, this potential conflation would work against confirming our hypothesis of functional inhibition, as this hypothesis required demonstrating different effects of alpha in periodic and aperiodic sites. As our results support an interaction between periodic/aperiodic sites and alpha power bins, we believe that the method we used is sufficient into sorting sites with predominantly periodic and aperiodic activity.

Third, we analyzed the relationship between BHA and power in a range of low frequencies (2–40 Hz). Thus, we overcome a limitation of some previous studies which only focused on a predefined frequency-band (e.g., alpha: Potes et al., 2014). We found that strong BHA occurred during states of weak power in the alpha+ band (i.e., alpha and neighboring frequencies including beta and theta), suggesting that the functional inhibition account is not exclusive to a narrowband alpha rhythm. While it is possible that frequencies around the alpha band may reflect a similar function, it is important to highlight that the relationship between ongoing power and BHA was more prominent and sustained in time within the alpha band (Fig. 2). Additionally, it is possible that analysis techniques such as frequency smoothing may have contributed to the spreading of the effect beyond the alpha band. Finally, we found that ongoing delta-band power (<4 Hz) was unrelated to BHA (Fig. 2FG), suggesting that the relationship between BHA and low-frequency power was unlikely determined by a change of the slope of the aperiodic signal affecting all low frequencies (including delta). This finding is particularly important as it further demonstrates that the relationship between alpha oscillations and BHA reflects a true oscillatory modulation.

Fourth, we analyzed how predictability cues influenced prestimulus alpha power and BHA in syllable-locked epochs. We found that predictions decreased the power of alpha oscillations (in periodic sites) before syllable onset, consistent with previous studies (Rohenkohl and Nobre, 2011; van Diepen et al., 2015; but see Mayer et al., 2016). Additionally, we found that predictions increased prestimulus BHA. We propose this pattern of results — decreased alpha power and increased BHA — reflects increased excitability in anticipation of the task-relevant target stimulus induced by predictions. Accordingly, this finding demonstrates a task-related/top-down modulation of alpha oscillations and BHA in line with the functional inhibition hypothesis.

In sum, these findings confirm the functional inhibition account and extend previous work by establishing the anatomical, temporal, and spectral characteristics of the relationship between alpha oscillations and neuronal excitability.

### 3.2. Relationship between prestimulus alpha power and poststimulus excitability

Based on the functional inhibition account, we hypothesized that states of strong prestimulus alpha oscillations are followed by low neuronal excitability during stimulus processing (i.e., in the poststimulus window). We found that states of strong alpha power were followed by a reduction in BHA during both the processing of visual and auditory

stimuli, as well as across sensory and non-sensory regions, suggesting that this phenomenon reflects a general property of alpha oscillations. These results are consistent with functional inhibition and with previous studies showing that ongoing alpha power is negatively correlated with the BOLD signal in sensory and non-sensory areas (Becker et al., 2008; Scheeringa et al., 2011; Walz et al., 2015) and early ERP components (Baslar and Stampfer, 1985; Becker et al., 2008; Iemi et al., 2019; Jasiukaitis and Hakerem, 1988; Rahn and Başar, 1993; Roberts et al., 2014). It is important to note the inhibitory effect of alpha oscillations was somewhat weaker during the early peak of the poststimulus BHA response in sensory ROIs. This is possibly due to a ceiling effect on BHA estimates driven by supra-threshold stimulation, or to the sparse electrode coverage of primary visual and auditory areas, preventing us from observing potential effects on early sensory responses.

By contrast, several previous studies have revealed a mixed pattern of results, showing a positive (Barry et al., 2000; Baslar and Stampfer, 1985; Becker et al., 2008; Dockree et al., 2007; Jasiukaitis and Hakerem, 1988; Mo et al., 2011; Roberts et al., 2014) or non-linear relationship (Kloosterman et al., 2019) between ongoing alpha power and other measures of poststimulus excitability (e.g., neuronal firing, non-invasive high-frequency power, and late ERP components). One possible explanation for these mixed results is that this relationship may depend on mechanisms other than functional inhibition. For example, ERPs are thought to reflect (1) stimulus-related neural activation, which is presumably suppressed during functional inhibition, and (2) baseline shift of non-zero-mean oscillations (Nikulin et al., 2007; Mazaheri and Jensen, 2008), which results in ERP amplification during states of strong prestimulus alpha power (Iemi et al., 2019). Accordingly, to rule out the possibility that the observed relationship between alpha oscillations and BHA was due to baseline shift, we estimated how BHA and ERPs were related to prestimulus alpha power separately for periodic sites with positive and negative oscillatory mean within the alpha band. We found that states of strong prestimulus negative-mean alpha oscillations were related to a more negative prestimulus ERP baseline and, in turn, a more positive poststimulus ERP signal. By contrast, states of strong prestimulus positive-mean alpha oscillations were related to a more positive prestimulus ERP baseline and, in turn, a more negative poststimulus ERP signal. In other words, states of strong prestimulus power were associated with a non-zero prestimulus ERP baseline, resulting in an amplification of the poststimulus ERP (in absolute value), consistent with baseline shift and with previous studies using non-invasive electrophysiology (Becker et al., 2008; Iemi et al., 2019). These results demonstrate that baseline shift contributes to the generation of the ERP (Nikulin et al., 2007). By contrast, BHA decreased with prestimulus alpha power regardless of the polarity of the oscillatory mean. Therefore, we conclude that the alpha-BHA relationship reflects an interaction between oscillatory activity and excitability consistent with functional inhibition, rather than a consequence of baseline shift.

Finally, it should be noted that, to maximize the number of trials for within-subject analysis, we used all trials regardless of whether or not the stimulus onset or content could be predicted based on the preceding cues (see Methods). While ongoing fluctuations in prestimulus activity before the (task-irrelevant) noise image reflect changes in internal processes including attention, arousal, or motivation, fluctuations before the other (task-relevant) visual cues and the target syllable may also reflect changes in predictability. Future studies are necessary to differentiate how these different endogenous processes modulate ongoing neural activity and behavior.

### 3.3. Relationship between prestimulus alpha power and behavior

Based on the functional inhibition account, we hypothesized that prestimulus alpha oscillations modulate task performance (e.g., RTs in the auditory discrimination task). We found slower RTs following states of strong prestimulus alpha power estimated in the window before the task-relevant target stimulus (i.e., in syllable-locked epochs) across both periodic and aperiodic sites, including auditory and somatomotor regions. It is important to note that previous studies reported both positive (Bollimunta et al., 2008; Bompas et al., 2015; Kelly and O'Connell, 2013; Kirschfeld, 2008; Lou et al., 2014; Mazaheri et al., 2014; Min and Herrmann, 2007; Paoletti et al., 2019; van den Berg et al., 2016; Zhang et al., 2008), negative (Bollimunta et al., 2008; Del Percio et al., 2007; Zhang et al., 2008), and null relationships (Andino et al., 2005; van Dijk et al., 2008; Bays et al., 2015) between prestimulus alpha power and RTs. This mixed evidence may be due to whether power is estimated in a brain region processing task-relevant or -irrelevant information, as well as to task differences (e.g., whether accuracy or speed is emphasized), different laminar organization across regions (Bollimunta et al., 2008, 2011; Mo et al., 2011), or to long-range temporal dependencies in both alpha power and RT estimates, resulting in spurious positive and negative correlations (Schaworonkow et al., 2015).

Interestingly, we observed that RTs were positively related to alpha power in periodic sites, but also to the aperiodic signal in the same frequency band (i.e., alpha power in aperiodic sites). This may be explained by residual periodic activity in individual trials in aperiodic sites, or by a recent proposal (Donoghue et al., 2020; Peterson et al., 2018) suggesting that, in addition to alpha oscillations, the aperiodic signal modulates information processing and thus behavior (e.g., RT: Zhang et al., 2008).

### 3.4. Interrelation between prestimulus alpha power, behavior, and excitability

Based on the functional inhibition account, we hypothesized that prestimulus alpha oscillations influence behavior by modulating excitability during stimulus processing. Therefore, key to our analysis was the mediation between prestimulus alpha power and behavior via poststimulus BHA (Judd and Kenny, 1981). We found that in periodic sites (1) single-trial prestimulus alpha power was negatively correlated with poststimulus BHA, and (2) positively correlated with RTs (consistent with our binning analysis), (3) even after controlling for poststimulus BHA; and (4) that single-trial poststimulus BHA was negatively correlated with RTs, (5) even after controlling for prestimulus alpha power. Critically, controlling for poststimulus BHA reduced the correlation between prestimulus alpha power and RTs (i.e., indirect effect) in periodic sites (but not in aperiodic sites), suggesting that alpha oscillations and BHA explained a similar portion of RT variability. This is consistent with mediation and indicates that the behavioral changes associated with alpha oscillations (rather than the aperiodic signal in the same band) are related to the influence of alpha on excitability.

Notably, some previous studies attempted to examine the interrelation between alpha oscillations, excitability, and behavior (e.g., Hartmann et al., 2015; Kayser et al., 2016; Vugt et al., 2018). Some analyzed concurrent neural and behavioral changes as a function of ongoing/prestimulus alpha power, without directly assessing their interrelation (Bollimunta et al., 2008; Haegens et al., 2011; Min and Herrmann, 2007; Mo et al., 2011; Vugt et al., 2018). Other studies used statistical methods to directly test for said interrelation, but the results were null or inconclusive, possibly because excitability was estimated with indirect/non-invasive measures (stimulus-evoked response: Wöstmann et al., 2019; decoding metric: Kayser et al., 2016; McNair et al., 2019). Accordingly, to the best of our knowledge, our study is the first to show that a modulation of poststimulus excitability mediates the relationship between prestimulus alpha oscillations and behavior, consistent with functional inhibition. However, it is important to note that our results do not allow us to distinguish whether the mediation reflects a direct effect of alpha oscillations, or a consequence of an additional process affecting all variables in parallel. Future research should address this question by testing whether alpha oscillations directly cause the mediation effect, ideally by using neuromodulation techniques (Helfrich et al., 2014; Romei et al., 2010).

### 3.5. Relationship between prestimulus alpha power and neural stimulus feature encoding

Based on the functional inhibition account, we hypothesized that prestimulus alpha oscillations affect how stimulus information is encoded in excitability measures (i.e., poststimulus BHA). Using BHA temporal patterns, we estimated decoder accuracy and confidence across different states of prestimulus alpha power and between periodic and aperiodic sites. We found that decoder confidence decreased with alpha power most prominently in periodic sites with a negative alpha-BHA relationship. This is consistent with the functional inhibition account and suggests that the BHA reduction during states of strong alpha power may underlie the decrease in decoder confidence. By contrast, across all sites, decoder accuracy was unaffected by prestimulus alpha power, even after controlling for overall decoder accuracy and for the alpha-BHA relationship.

How could the decoder indicate higher confidence without becoming more accurate during states of increased excitability? We speculate that weak prestimulus alpha power is associated with higher BHA responses, but also with proportionally more variability, leaving the signal-to-noise ratio (i.e., mean-to-variance ratio, or Fano factor) unchanged (Goris et al., 2014; Tolhurst et al., 1981; Tomko and Crapper, 1974). However, as mean and variance of the neural response increase, the neural stimulus representations fall farther from the classifier's discriminant boundary or hyperplane (see model in Fig. 5F). This modulation is expected to affect the overall strength of neural stimulus representations (i.e., decoder confidence) for both correct, but also incorrect trials, without affecting their precision (i.e., decoder accuracy). Future work is necessary to determine whether the effects of alpha oscillations on the magnitude of neuronal excitability are multiplicative (as assumed in our model) or additive, and whether they are proportional to changes in response variability, ideally by using single-unit recordings which enable an estimation of spike mean and variability.

Our findings that prestimulus alpha oscillations affect decoder confidence, not accuracy, are consistent with a growing number of studies reporting that strong prestimulus alpha oscillations are related to reduced subjective, rather than objective measures of perceptual decision-making in both detection (less liberal criterion: Iemi et al., 2017; Limbach and Corballis, 2016) and discrimination tasks (lower visibility: Benwell et al., 2017, 2021; lower confidence: Samaha et al., 2017). Future research is necessary to establish whether lower decoder confidence, reflecting decreased stimulus encoding strength, underlies the perceptual effects in these studies.

Previous studies have analyzed how decoding performance is related to alpha oscillations, though the results were inconsistent, showing positive (Kayser et al., 2016; McNair et al., 2019), negative (Barne et al., 2020; van Ede et al., 2018), and null relationships (Griffiths et al., 2019). In the studies reporting a positive relationship, stimulus features were decoded using low-frequency EEG activity (1–70 Hz), which includes alpha oscillations. Therefore, it is possible that high signal-to-noise ratio may result in strong alpha power estimates as well as higher decoding performance, potentially leading to a spurious positive correlation. To avoid such circularity, in other previous studies stimulus identity was decoded using the hemodynamic fMRI BOLD signal (Griffiths et al., 2019) or the low-frequency activity after removing alpha-band activity (van Ede et al., 2018). In our study, we addressed this issue by applying decoding analysis on poststimulus BHA, which does not include the alpha band, and reflects a more direct excitability measure than the fMRI signal. We reasoned that any relationship between alpha oscillations and decoding performance would reflect a genuine modulation of stimulus encoding, rather than a consequence of a potentially circular analysis.

It is important to note that we found no significant effect of prestimulus alpha power on decoder accuracy, consistent with one previous report using representational similarity analysis (Griffiths et al., 2019). By contrast, one previous study (van Ede et al., 2018) found that lower decoder accuracy (i.e., Mahalanobis distance) was related to strong prestimulus alpha power in posterior EEG, specifically in the presence of poststimulus distractors. When distractors were absent (as in our paradigm), decoder accuracy was no longer related to prestimulus alpha power, suggesting that the effect on decoder accuracy might emerge when the task requires the suppression of task-irrelevant information, which is believed to be supported by alpha oscillations (Haegens et al., 2010). Moreover, in another study (Barne et al., 2020), lower decoder accuracy (i.e., AUC) was related to strong prestimulus alpha power in parieto-occipital EEG electrodes when attention was cued to the spatial location of the to-be-decoded sensory stimuli. Therefore, it is possible that decoder accuracy may be affected by attention-induced/local (as opposed to ongoing/global) fluctuations of alpha oscillations. Accordingly, future studies are necessary to determine whether decoder accuracy is influenced by a top-down modulation of alpha oscillations, ideally by using paradigms manipulating distractors and spatial attention.

Of note, in this study we performed spatial decoding, which uses temporal features of the neural signal at each recording site to classify sensory stimuli. This enabled us to combine data across patients and carry out group-level, across-site statistical testing. An alternative to spatial decoding is temporal decoding, which instead uses spatial features of the neural signal at each time point. Temporal decoding is more common in non-invasive electrophysiology where the data is collected at similar spatial locations across subjects, allowing for group-level, across-subject statistical testing. In the current study, the different electrode coverages across patients, together with the low sample size, prevents us from performing temporal decoding. Future studies using non-invasive electrophysiology with a bigger sample size are necessary to test how temporal decoding is affected by ongoing oscillations.

### 3.6. Conclusions

In sum, we demonstrate that strong prestimulus oscillations in the alpha+ band (i.e., alpha and neighboring frequencies), rather than the aperiodic signal, are associated with (1) decreased BHA (i.e., low neuronal excitability) before and after sensory input. Furthermore, we show that strong prestimulus alpha oscillations result in (2) slower perceptual decisions, and (3) reduced sensory encoding strength. These results provide a link between neural oscillations, excitability, and task performance, consistent with functional inhibition: we propose that, by modulating neuronal excitability, ongoing alpha+ oscillations affect behavior and neural stimulus representations.

## 4. Methods

### 4.1. Participants

This study involved nine individuals with medication-resistant epilepsy (5 females; mean age, 29 years, SEM=4). All patients had intracranial electrodes implanted as part of presurgical diagnosis of epilepsy. Data collection was performed at the Comprehensive Epilepsy Center of New York University Langone Health, and was approved by the Institutional Review Board at New York University Langone Health. Verbal and written informed consent were collected from all patients before participation in the study in accordance with the Declaration of Helsinki. Results from six individuals have been previously reported (Auksztulewicz et al., 2018).

### 4.2. Experimental design

Each trial started with the presentation of a fixation cross (1.5 to 2 s), followed by a sequence of visual and auditory stimuli: a noise image, a picture of a scene, a picture of a face, and an auditory syllable (Fig. 1A). The order of the sequence was fixed across trials. Each of the visual stimuli and the auditory stimulus were presented for a duration of 0.210 and 0.250 s, respectively. Visual stimuli were displayed

at the center of a laptop screen placed at the bedside at approximately a 70-cm distance. The noise image consisted of grayscale random horizontal and vertical lines and was identical in all trials. For the other stimuli, different exemplars were presented across trials, selected from four different scene images (e.g., the White House or Taj Mahal), eight different face images (e.g., Barack Obama, George W Bush), and two different syllables (/ga/ vs. /pa/) The target syllables were produced by a male speaker; during the experiment, they were played with speakers at 70 dB or levels comfortable for the patient. The participants were asked to perform a 2-alternative-forced-choice discrimination of the target syllable ("which syllable did you hear: /ga/ vs. /pa/?") with a speeded button press using the index and middle fingers of the right hand. The experiment was implemented in Presentation (Neurobehavioral Systems; https://www.neurobs.com/).

The behavioral paradigm was based on a 2 × 2 factorial design with factors "when" predictability and "what" predictability, resulting in four different conditions, each of which was recorded in a separate run, and randomized across participants (for more information see Auksztulewicz et al., 2018). In brief, "when" predictability was manipulated by varying the timing between visual and auditory stimuli across trials: the four stimuli comprising a trial were presented with either a fixed inter-stimulus interval (ISI) of 1 s in the temporally predictable runs or with a randomly jittered ISI (mean 1 ± 0 to 0.5 s random jitter) across trials in the temporally unpredictable runs. In addition, "what" predictability was manipulated by using contingencies between the visual stimuli and the target syllable. In the content-predictable runs, specific sequences of scene/face images predicted the identity of the target syllable (75% probability), while in the content-unpredictable runs, the two target syllables were equiprobable across trials. To increase statistical power of single-trial analyses, we combined trials from all predictability conditions with a sufficient prestimulus window (i.e., trials with ISI >= 1 s).

### 4.3. Neural recordings

The electrodes consisted of 8 × 8 grids of subdural platinum-iridium electrodes embedded in Silastic sheets (2.3-mm-diameter contacts, AdTech Medical Instruments) with a minimum 10-mm center-to-center distance implanted over the temporal/frontal cortices, with additional linear strips of electrodes and/or depth electrodes. In this dataset, grid, strip and depth-electrodes were used at 41, 43, 16% of the sites, respectively (total $N = 1044$ electrodes). Recordings were obtained using the Nicolet ONE clinical amplifier (Natus). During recording, the signal was bandpass filtered from 0.5 to 250 Hz, digitized at 512 Hz, and online referenced to a screw bolted to the skull.

We performed electrode localization using previously described procedures (Yang et al., 2012). In brief, for each patient, we obtained preoperative and postoperative T1-weighted MRIs, which were subsequently co-registered and normalized to an MNI-152 template, allowing the extraction of the electrode location in MNI space. We assigned anatomical labels to each electrode using FreeSurfer cortical parcellation (Fischl et al., 2004) based on the Desikan-Killiany atlas (Desikan et al., 2006), resulting in 983 localized electrodes out of 1044. The Freesurfer suite provides an automated labeling of the cerebral cortex into units based on gyral and sulcal structure.

Electrophysiological data analysis was performed using custom-built MATLAB code (version R2019a; The MathWorks; RRID:SCR_001622) and the Fieldtrip toolbox (version 2018.08.01; www.ru.nl/neuroimaging/fieldtrip). Continuous signals were notch-filtered at 58–62 Hz and harmonics using zero-phase Butterworth filters. The data were re-referenced to a common average and segmented into epochs from −1.5 to 1 s relative to the onset of each visual and auditory stimulus (stimulus-locked) and relative to the motor response (response-locked epochs). In total, we obtained 96(trials)*5(epochs)*4(runs) = 1920 epochs per patient.

We rejected artifactual electrodes in which the BHA time-course during the 1-s prestimulus window exceed 5 standard deviations from the mean in at least 50 trials. We corroborated this automatic procedure with visual inspection and removed a total of 76 artifactual electrodes across 9 patients.

We discarded 48 epochs per patient with an ISI <1 s. Additionally, we rejected artifactual epochs in which either the raw signal or the BHA time-course (at any electrode) from −1 to 1 s relative to stimulus onset exceeded 25 standard deviations from the mean. We corroborated this automatic procedure with visual inspection and removed 136 artifactual epochs per patient. We analyzed 1595 epochs per patient (344 noise-locked, 278 scene-locked, 281 face-locked; 356 syllable-locked; 334 response-locked epochs). For RT and single-trial analysis (mediation and decoding), we further discarded noise- and syllable-locked epochs with incorrect responses (36 epochs per patient), and with premature (RT<0.1 s; 10 epochs per patient) or late RTs (RT > 0.8 s; 37 epochs per patient). Mean RT across patients was 0.466 s (SEM 0.031).

### 4.4. Spectral analysis

We computed power spectra for time windows before and after stimulus onset, separately for each electrode and for noise-, scene-, face, and syllable-locked epochs. The duration of the prestimulus window was 1 s for noise- and syllable-locked epochs, and 0.5 s (zero-padded to 1 s) for scene- and face-locked epochs to diminish the contamination due to event-related activity of previous visual stimuli. The duration of the poststimulus window was 1 s in all epochs. We multiplied these epochs with a Hanning taper, and estimated the spectra between 1 and 150 Hz (1-Hz frequency resolution) using a fast Fourier transform (FFT) approach.

We computed a single-trial estimate of the power in the alpha (7–14 Hz) and BHA range (70–150 Hz). Note that the lower bound for BHA was set to 70 Hz based on previous literature (e.g.,: Leszczyński et al., 2020) to exclude narrow-band gamma oscillations occurring between 30 and 70 Hz, which reflect distinct physiological phenomena. To avoid disproportionally representing power at the lower-bound frequencies (~70 Hz) due to the 1/f property of the neural signal, we computed the percent signal change relative to the mean power across trials separately for each frequency and site and then averaged the values between 70 and 150 Hz to obtain a frequency-normalized estimate of BHA. This normalization ensures that frequencies between 70 and 150 Hz equally contribute to the BHA estimates.

In addition, to inspect the time course of the spectral dynamics, we computed time-frequency representations (TFRs) of power. We estimated the low-frequency TFR (2–40 Hz; 1-Hz step size) using an adaptive sliding time window of three cycles length ($\Delta t = 3/f$), and the high-frequency TFR (70–150 Hz; 5-Hz step size) using a fixed window of 0.2 s, and applied a Hanning taper before estimating power using an FFT approach. The BHA time-course was computed by averaging the high-frequency TFR across frequencies.

### 4.5. Spectral peak detection

To determine the individual alpha peak frequency for each site, we used the local maximum method whereby we detected the highest local maximum within the alpha range of the power spectra (using 1-s prestimulus noise-locked epochs), regardless of its absolute magnitude (no power threshold used; following the methods in Haegens et al., 2014). We refer to electrodes with and without alpha-band peaks as "periodic" and "aperiodic" sites, respectively. Note that the alpha range was set between 7 and 14 Hz in line with previous literature and to account for slower alpha oscillations previously reported in epilepsy patients (Stoller, 1949; Abela et al., 2019).

In addition to the local maximum peak detection method described above, we used four complimentary methods to classify the sites into periodic and aperiodic based on activity during the 1-s prestimulus

noise-locked epochs. First, we used linear regression (least-squares fit) to fit a linear model to the log-transformed power spectra separately for each site. We subtracted the fitted linear trend from the log-transformed power spectra to remove the 1/f aperiodic signal, as this obscures smaller peaks by strongly biasing lower frequencies. We then detected the alpha-band peak on the flattened power spectrum using the same method reported above (Haegens et al., 2014; Nikulin & Brismar, 2006) and sorted the sites into periodic (with peak) and aperiodic (without peak). We found 542 periodic sites (81% overlap with local maximum method) and 502 aperiodic sites (83% overlap with local maximum method).

Second, we applied an adaptive algorithm fitting a Gaussian curve to the power spectra separately for each site. We used the fitted gaussian curves to detect peaks within the alpha range (Van Albada and Robinson, 2013) and sorted the sites into periodic (with peak) and aperiodic (without peak). We found 469 periodic sites (94% overlap with local maximum method) and 575 aperiodic sites (85% overlap with local maximum method). Since the gaussian fit effectively smooths the spectra, this method is thought to improve peak detection, for example, when the spectrum has two local maxima close to each other, or when noisy spectra lead to spurious peaks. Moreover, peak detection is more conservative using this method as sites without substantial modulation in the alpha range are automatically excluded (i.e., Gaussian fit fails). Therefore, this enables us to confirm that our original peak detection method was not biased by inclusion of potentially spurious peaks.

Third, we used the Fitting Oscillations & One Over F (FOOOF) algorithm (Voytek et al., 2015; Donoghue et al., 2020) to detect alpha-band peaks as frequency regions of the power spectrum within the alpha range with power over and above the aperiodic 1/f signal. We used Welch's method to compute the power spectra separately for each site. Then, we applied the FOOOF algorithm to detect peaks within the alpha range and sorted the sites into periodic (with peak) and aperiodic (without peak). We selected the following settings based on the FOOOF online tutorial and related publications (modeled frequencies: 2–40 Hz, maximum number of peaks: 6, peak widths: 1–8, minimum peak height: 0.1 arbitrary units of power, peak threshold: 2 standard deviations, fixed approach). For each site, we estimated the error of the fit and excluded 45 sites where the error exceeded an arbitrary threshold (i.e., 2 standard deviations above the mean error across all sites), indicating that periodic and aperiodic activity could not be separated in these sites. The remaining sites had an average error of fit of 0.049 au (SEM=0.001); the error of fit did not significantly differ between periodic and aperiodic sites ($t(997)=-0.767$, $p = 0.443$). We found 737 periodic sites (59% overlap with local maximum method) and 262 aperiodic sites (74% overlap with local maximum method).

Fourth, we applied an extended version of the Better OSCillation detection method (eBOSC; cf. Caplan et al., 2001; Whitten et al., 2011, Kosciessa et al. 2020) to sort the sites in periodic and aperiodic. We first concatenated all epochs into one data segment, and performed time-frequency transformation using 6-cycle Morlet wavelets with 41 logarithmically-spaced center frequencies ranging from 2 to 64 Hz. We estimated the aperiodic signal using robust regression, excluding frequency within the alpha range. The power threshold (PT) was set to the 95% percentile of the robust fit of the aperiodic signal and the duration threshold (DT) was calculated based on the duration of three complete oscillation cycles at each frequency. Episodes of periodic activity (i.e., oscillations) were defined as time points during which the wavelet-derived power at a particular frequency exceeds both PT and DT. For each site and frequency, we estimated the proportion of time within the analyzed data segment during which oscillations at a given frequency were present (i.e., $P_{episode}$). We averaged $P_{episode}$ within the alpha range separately for each site and then sorted the sites into three bins based on the magnitude of alpha-band $P_{episode}$. We refer to the bins with strongest (average $P_{episode}$=0.354, SEM=0.004) and weakest alpha-band $P_{episode}$ (average $P_{episode}$=0.089, SEM=0.002) as periodic and aperiodic sites, respectively. We found 355 periodic sites (82% overlap with local maximum method) and 345 aperiodic sites (76% overlap with local maximum method). The sites from the middle bin (mean $P_{episode}$= 0.186, SEM= 0.002) were excluded from subsequent data analysis, as they reflect a mixture of periodic and aperiodic activity.

### 4.6. Power-based binning analysis

To analyze the across-trial relationship between low-frequency oscillations and BHA, for each site we sorted trials into five bins (e.g., Linkenkaer-Hansen et al., 2004; Iemi et al., 2019) based on alpha power (7–14 Hz) during the 1-s prestimulus windows. For each bin we computed the average BHA for each time window. Similarly, we binned trials based on BHA, and computed the average TFRs of low- and high-frequency power spectra per bin. For group-level statistical analysis and visualization, the power spectra were normalized by the average power across all frequencies and bins, while the TFRs and BHA time-courses were normalized by the average power across time and bins per frequency.

### 4.7. Statistical analysis

We used non-parametric cluster-based permutation tests (Maris and Oostenveld, 2007) for contrasts involving a temporal dimension. By clustering neighboring samples (i.e., time-frequency points) that show the same effect, this test controls for the multiple comparison problem while taking into account the dependency of the data. For each sample, a dependent-sample t-value was computed across sites for the relevant contrast (e.g., power difference between bins). We selected all samples for which this t-value exceeded an a priori threshold ($p < 0.05$), clustered these samples on the basis of temporal-spectral adjacency, and computed the sum of t-values within each cluster. By randomly permuting the data across the most extreme bins (bin 1 and 5) 1000 times and determining the maximum t-sum on each iteration, we obtained a reference distribution of t-sums. A final p-value was calculated as the proportion of t-sums under the null hypothesis larger than the sum of t-values within clusters in the observed data. We adjusted the final alpha thresholds using Bonferroni correction for multiple comparisons (i.e., for multiple contrasts).

### 4.8. Functional-anatomical regions of interest

We defined three experimentally relevant ROIs using a combination of functional and anatomical localizers. The functional localizer identified recording sites that were active during the presentation of the experimental stimuli (noise, scene, face, and syllable in stimulus-locked data) and during the behavioral response (in response-locked data). For each site we averaged the BHA time-course over the prestimulus window across stimulus-locked (−1.1 to −0.1 s) and response-locked epochs (−1.35 to −0.35 s). Then, for each site, we calculated the threshold as 2 standard deviations above the prestimulus BHA signal averaged across time points and trials. We identified stimulus-related and response-related sites as those sites whose poststimulus BHA time-course exceeded the site-specific threshold in stimulus-locked (0 to 0.5 s) and response-locked epochs (−0.25 to 0.25 s). Using this functional localizer, we identified 95 noise-related, 95 scene-related, 137 face-related, 300 syllable-related, and 565 response-related sites across 9 patients.

We complemented the functional localizer with an anatomical localizer. Specifically, we identified regions based on anatomical labels classically related to sensory processing and motor planning/response. Our visual localizer included the cuneus, lateral-occipital areas, lingual area, pericalcarine, fusiform gyrus, and inferior-temporal areas ($N = 123$ sites). Our auditory localizer included transverse-temporal area, middle-temporal, superior-temporal, banks of the superior-temporal sulcus, supramarginal areas, pars opercularis, pars triangularis, superior-temporal gyrus ($N = 309$). Our somatomotor localizer included precentral and postcentral areas ($N = 191$).

Finally, we combined the functional and anatomical localizers to obtain the visual, auditory and somatomotor ROIs. Specifically, the overlap between visual anatomical sites and the combination of noise-, scene-, face-related functional sites yielded the visual ROIs ($N = 68$). The overlap between the auditory anatomical sites and the syllable-related functional sites yielded the syllable-selective ROI ($N = 103$), while the overlap between the somatomotor anatomical sites and the response-related functional sites yielded the somatomotor ROI ($N = 129$).

### 4.9. Baseline shift analysis

To determine whether baseline shift of non-zero-mean alpha oscillations contributes to the observed alpha-BHA relationship in periodic sites, we estimated the non-zero-mean property of alpha oscillations using the Baseline Shift Index (BSI: Nikulin et al., 2007, V.V. 2010) and the Amplitude Fluctuation Asymmetry Index (AFAI: Mazaheri and Jensen, 2008, A. 2010; van Dijk et al., 2010). In each patient and for each site, BSI and AFAI were estimated on the continuous (i.e., non-epoched) data and averaged across experimental runs. We classified periodic sites in two groups depending on whether BSI (or AFAI) within the alpha range was positive or negative.

To quantify BSI, the raw EEG data was first band-pass filtered using a 4th-order Butterworth filter centered at each frequency of interest ±1 Hz. Then, the Hilbert transform was used to extract a time-resolved power envelope. In addition, the raw EEG data was low-pass filtered using a 4th-order Butterworth filter with a 3-Hz cut-off frequency. We computed BSI as the Spearman correlation ($\rho$) between the power envelope and the low-pass EEG signal (i.e., slowly varying DC-like component) separately for each frequency and site (Iemi et al., 2019). When the low-pass signal is unaffected by power fluctuations, resulting in BSI = 0, there is evidence for zero-mean oscillations. Instead, when states of strong power result in positive (BSI>0) or negative (BSI<0) shifts of the low-pass signal, there is evidence for positive and negative oscillatory mean, respectively.

AFAI is based on the assumption that power fluctuations of non-zero-mean oscillations affect the peaks and troughs of the EEG signal differently. To quantify AFAI, we identified the time points of peaks and troughs as those data samples in the band-passed data which were larger (peaks) and smaller (troughs) than the two neighboring samples, respectively, and then estimated the magnitude of the raw EEG signal at these time points. We computed AFAI as the normalized difference between the variance at the time points of the peaks and troughs in the raw EEG signal separately for each frequency and site. Amplitude symmetry (AFAI = 0, power fluctuations equally modulate peaks and troughs) indicates a zero oscillatory mean. Amplitude asymmetry indicates a non-zero-mean: specifically, AFAI>0 indicates a stronger modulation of the peaks relative to the troughs, or a positive oscillatory mean; AFAI<0 indicates a stronger modulation of the troughs relative to the peaks or a negative oscillatory mean (see V.V. Nikulin et al., 2010 for a comparison between BSI and AFAI).

We used a binning approach to analyze how BHA in the prestimulus and poststimulus window in noise-locked epochs changes as a function of prestimulus alpha power separately for the negative- and positive-mean sites. We repeated this analysis for ERPs: single-trial ERPs were computed on low-pass filtered data (<30 Hz) and baseline-corrected with the 1-s prestimulus signal.

### 4.10. Behavioral analysis

We estimated behavioral performance using reaction times (RTs). Note that discrimination accuracy was at ceiling (90% correct discrimination across blocks) with only 36 incorrect responses per patient, thus preventing an analysis of trial-by-trial fluctuations. We used a binning approach to analyze how RTs on correct trials change as a function of prestimulus alpha power in periodic and aperiodic sites. We log-transformed RTs to correct for the skewness of their distribution. We averaged RTs across epochs for each bin, and normalized these estimates by the average RT across all epochs, separately for each patient. This analysis was run for noise- and syllable-locked epochs.

To understand the interrelation between prestimulus oscillations, behavior, and poststimulus excitability in syllable-locked epochs, we tested a mediation model in which prestimulus alpha oscillations (independent variable X) may affect RTs on correct trials (dependent variable Y) via a modulation of poststimulus BHA (mediator, M). To this end, we used a causal step approach (Baron and Kenny, 1986; MacKinnon et al., 2000, 2007; Judd and Kenny, 1981) characterized by analyzing the correlation coefficients of four generalized linear models (GLMs).

The first GLM consists of a simple regression with independent variable predicting the mediator: $M = i + aX + e$, where X is prestimulus alpha power, M is poststimulus BHA, and a is the zero-order correlation coefficient reflecting the direct effect between X and M. In all GLMs, i refers to the intercept and e to the residual error of the model. Mediation requires that prestimulus alpha power is negatively correlated with poststimulus BHA ($a < 0$).

The second GLM consists of a simple regression with the mediator variable predicting the dependent variable: $Y = i + bM + e$, where Y is RT, M is poststimulus BHA, and b is the zero-order correlation coefficient reflecting the direct effect between Y and M. Mediation requires that poststimulus BHA is positively correlated with RTs ($b < 0$).

The third GLM consists of a simple regression with the independent variable predicting the dependent variable: $Y = i + cX + e$, where X is prestimulus alpha power, Y is RT, and c is the zero-order correlation coefficient reflecting the direct effect between X and Y. Mediation requires that prestimulus alpha power is positively correlated with RTs ($c > 0$).

The fourth GLM consists of a multiple regression with the independent variable and the mediator predicting the dependent variable: $Y = i + c'X + b'M + e$, where X is prestimulus alpha power, Y is RTs, M is poststimulus BHA, and c' and b' are the partial correlation coefficients reflecting the indirect effect between X and Y adjusted for M, and between M and Y adjusted for X, respectively. Mediation requires that poststimulus BHA is positively correlated with RTs after controlling for prestimulus alpha power ($b' < 0$).

In addition, mediation requires a significant reduction in the effect of the independent variable on the dependent variable after accounting for the mediator, which can be estimated by the difference between zero-order and partial coefficients ($c - c'$): $c > c'$ (in absolute values) indicates partial mediation (or full mediation if $c' = 0$). Note that mediation assumes that the independent variable X causes the mediator M (second GLM), and thus that the two variables are correlated. This correlation results in multicollinearity when the effects of independent variable and mediator on the dependent variable are estimated in a multiple regression model, yielding reduced coefficients in the fourth GLM.

We ran these four GLMs separately for each site, using single-trial FFT estimates of prestimulus alpha power, frequency-normalized poststimulus BHA, and RTs. Direct effects were estimated using variables that were normalized by z-scoring across trials, whereas the indirect effect was estimated using the original variables (i.e., not normalized). Note that, to compute unstandardized coefficients of the first and fourth GLM, we used RTs expressed in ms.

### 4.11. Decoding analysis

We used multivariate pattern analysis (or "decoding") to examine the relationship between prestimulus alpha oscillations and neural stimulus representations encoded in BHA. First, we tested whether stimulus features (i.e., syllable identity) could be decoded from the recorded neural activity; next we tested whether prestimulus alpha power modulates decoder accuracy and/or confidence.

We evaluated stimulus encoding in the time-course of neural activity using spatial decoding (similar to Gwilliams and King, 2020): we used l2-regularized logistic regression, under a stratified k-fold ($k = 4$) cross validation scheme. Input features were normalized by the mean

and the standard deviation of the training set. All decoding analyses were performed using the Python package scikit-learn (version 0.22.1: Pedregosa et al., 2011). The optimal regularization parameter was selected for each fold separately, by finding which of 10 log-spaced regularization strengths from 1e-4 to 1e+4 led to best model performance on the test set (using the LogisticRegressionCV scikit-learn function with default parameters). We used 1000 maximum iterations of the 'lbfgs' optimization algorithm. The input features to the classifier were 17 time-samples (0 to 0.8 s relative to syllable onset) of either BHA (frequency-normalized estimate) or the low-passed signal (< 30 Hz; e.g., Gwilliams and King, 2020; King et al., 2016; Salti et al., 2015). We downsampled the low-passed signal to match the temporal resolution of BHA. The categorical class labels corresponded to syllable identity (/ga/ vs. /pa/). We analyzed 310 trials for each patient, with 233 trials used for each training set and 76 for each test set. The model was trained and tested within each recording site separately, providing a prediction for each trial at each location over space, based on the multivariate pattern of activity over time.

We derived two decoding performance metrics from the classifier predictions: AUC (i.e., decoder accuracy) and the maximum probabilistic prediction (i.e., decoder confidence). For AUC, we evaluated the similarity between the true label categories of the test set and the probabilistic class labels (normalized distance from the fit hyperplane: "predict_proba" in scikit-learn) of the same trials. We computed the AUC under the null hypothesis by randomly shuffling the label categories to the classifier and obtained a p-value as the proportion of the null AUC estimates (across sites) that exceeded the true AUC independently for each site. We considered the AUC as significantly greater than chance if its p-value < 0.05. This analysis resulted in a decoding anatomical map indicating where syllable identity can be linearly decoded from temporal patterns of either BHA or low-passed signal (Fig. 5AB supplement). The maximum probabilistic prediction indicates the strength of the neural stimulus representation, regardless of whether or not it matches the ground truth; in other words, it is a measure of the classifier's "confidence" about the true class label of a given trial, regardless of accuracy. When the probability = 0.5, the classifier's predictions for the two class labels are identical (i.e., low confidence); when probability > 0.5, the classifier prediction for one class label is stronger than for the other class label (i.e., higher confidence).

We asked whether prestimulus oscillatory state shapes neural stimulus representations as reflected by decoding performance metrics. To test this, we evaluated how decoder accuracy and confidence based on BHA was related to trial-by-trial fluctuations of prestimulus alpha power. We used the classification procedure explained above, replacing the k-fold cross validation with a leave-one-out cross-validation (LOOCV) procedure. In LOOCV, the classifier is fit on all trials but one, evaluating model performance on the remaining "left-out" trial as a single-item test set. This is advantageous because it allows a maximal amount of data to be used for training, thus reducing noise in the model fit, and because it provides a single-trial decoding estimate which can be analyzed by a binning approach. For each site and test trial, we computed the probabilistic estimates of the logistic regression for each syllable, grouping the results into five bins relative to prestimulus alpha power. Then, for each bin we estimated the AUC using the classifiers' probabilistic estimates of the test trials and the vector of true class labels. Additionally, we normalized the maximum probabilistic estimates by z-scoring across trials, and computed decoder confidence by averaging these estimates within each bin.

## Credit authorship contribution statement

**Luca Iemi:** Conceptualization, Methodology, Software, Validation, Formal analysis, Data curation, Writing – original draft, Writing – review & editing, Visualization, Project administration. **Laura Gwilliams:** Software, Writing – review & editing. **Jason Samaha:** Conceptualization, Writing – review & editing. **Ryszard Auksztulewicz:** Investigation, Resources. **Jean-Remi King:** Software, Writing – review & editing. **Charles E Schroeder:** Supervision, Resources, Writing – review & editing, Funding acquisition. **Lucia Melloni:** Investigation, Resources, Funding acquisition. **Saskia Haegens:** Conceptualization, Methodology, Supervision, Resources, Writing – review & editing, Project administration, Funding acquisition.

## Data and code availability

Due to privacy issues of clinical data, the raw dataset for this study cannot be made openly available. The code to reproduce the results will be made available upon reasonable request.

## Acknowledgments

This work was supported by a grant from the Netherlands Organization for Scientific Research (NWO 016.Vidi.185.137, to S.H.), by the Silvio O Conte Center for Active Sensing (P50 MH109429, to L.I., C.E.S., S.H.), by the Basic Research Program of the National Research University Higher School of Economics (to V.V.N.), by the European Commission's Marie Skłodowska-Curie Global Fellowship (750459 to R.A.), by a grant called Finding A Cure for Epilepsy and Seizures (FACES, to O.D.), by a NIH grant (1R01EB019805 to T.T), by the NYU Abu Dhabi Institute (G1001 to L.G.), by the William Orr Dingwall Dissertation Fellowship (L.G.), by a NIH re-entry supplement (R01DA038154, to Y.M.C), and by a Marie Curie International Outgoing Fellowship within the 7th European Community Framework Programme (L.M.).

We thank Esra Al, Julio Rodriguez Larios, Elie Rassi, and Hesham ElShafei for helpful comments on the manuscript.

## Supplementary materials

Supplementary material associated with this article can be found, in the online version, at doi: 10.1016/j.neuroimage.2021.118746.

## References

Abela, E., Pawley, A.D., Tangwiriyasakul, C., Yaakub, S.N., Chowdhury, F.A., Elwes, R.D.C., Brunnhuber, F., Richardson, M.P., 2019. Slower alpha rhythm associates with poorer seizure control in epilepsy. Ann. Clin. Transl. Neurol. 6 (2), 333–343. doi:10.1002/acn3.710.

Andino, S.L.G., Michel, C.M., Thut, G., Landis, T., Peralta, R.G.de, 2005. Prediction of response speed by anticipatory high-frequency (gamma band) oscillations in the human brain. Hum. Brain Mapp. 24 (1), 50–58. doi:10.1002/hbm.20056.

Auksztulewicz, R., Schwiedrzik, C.M., Thesen, T., Doyle, W., Devinsky, O., Nobre, A.C., Schroeder, C.E., Friston, K.J., Melloni, L., 2018. Not all predictions are equal: "what" and "when" predictions modulate activity in auditory cortex through different mechanisms. J. Neurosci. 38 (40), 8680–8693. doi:10.1523/JNEUROSCI.0369-18.2018.

Barne, L.C., de Lange, F.P., Cravo, A.M., 2020. Prestimulus alpha power is related to the strength of stimulus representation. Cortex 132, 250–257. doi:10.1016/j.cortex.2020.08.017.

Baron, R.M., Kenny, D.A., 1986. The moderator–mediator variable distinction in social psychological research: conceptual, strategic, and statistical considerations. J. Pers. Soc. Psychol. 51 (6), 1173–1182. doi:10.1037/0022-3514.51.6.1173.

Barry, R.J., Kirkaikul, S., Hodder, D., 2000. EEG alpha activity and the ERP to target stimuli in an auditory oddball paradigm. Int. J. Psychophysiol. 39 (1), 39–50. doi:10.1016/S0167-8760(00)00114-8.

Baslar, E., Stampfer, H.G., 1985. Important associations among eeg-dynamics, event-related potentials, short-term memory and learning. Int. J. Neurosci. 26 (3–4), 161–180. doi:10.3109/00207458508985615.

Bauer, M., Oostenveld, R., Peeters, M., Fries, P., 2006. Tactile spatial attention enhances gamma-band activity in somatosensory cortex and reduces low-frequency activity in parieto-occipital areas. J. Neurosci. 26 (2), 490–501. doi:10.1523/JNEUROSCI.5228-04.2006.

Bays, B.C., Visscher, K.M., Le Dantec, C.C., Seitz, A.R., 2015. Alpha-band EEG activity in perceptual learning. J. Vis. 15 (10). doi:10.1167/15.10.7.

Becker, R., Reinacher, M., Freyer, F., Villringer, A., Ritter, P., 2011. How ongoing neuronal oscillations account for evoked fMRI variability. J. Neurosci. 31 (30), 11016–11027. doi:10.1523/JNEUROSCI.0210-11.2011.

Becker, R., Ritter, P., Villringer, A., 2008. Influence of ongoing alpha rhythm on the visual evoked potential. Neuroimage 39 (2), 707–716. doi:10.1016/j.neuroimage.2007.09.016.

Benwell, C.S.Y., Coldea, A., Harvey, M., Thut, G., 2021. Low pre-stimulus EEG alpha power amplifies visual awareness but not visual sensitivity. Eur. J. Neurosci. 00, 1–16. doi:10.1111/ejn.15166.

Benwell, C.S.Y., Keitel, C., Harvey, M., Gross, J., Thut, G., 2018. Trial-by-trial co-variation of pre-stimulus EEG alpha power and visuospatial bias reflects a mixture of stochastic and deterministic effects. Eur. J. Neurosci. 48 (7), 2566–2584. doi:10.1111/ejn.13688.

Benwell, C.S.Y., London, R.E., Tagliabue, C.F., Veniero, D., Gross, J., Keitel, C., Thut, G., 2019. Frequency and power of human alpha oscillations drift systematically with time-on-task. Neuroimage 192, 101–114. doi:10.1016/j.neuroimage.2019.02.067.

Benwell, C.S.Y., Tagliabue, C.F., Veniero, D., Cecere, R., Savazzi, S., Thut, G., 2017. Prestimulus EEG power predicts conscious awareness but not objective visual performance. eNeuro 4 (6). doi:10.1523/ENEURO.0182-17.2017.

Bollimunta, A., Chen, Y., Schroeder, C.E., Ding, M., 2008. Neuronal mechanisms of cortical alpha oscillations in awake-behaving macaques. J. Neurosci. 28 (40), 9976–9988. doi:10.1523/JNEUROSCI.2699-08.2008.

Bollimunta, A., Mo, J., Schroeder, C.E., Ding, M., 2011. Neuronal mechanisms and attentional modulation of corticothalamic alpha oscillations. J. Neurosci. 31 (13), 4935–4943. doi:10.1523/JNEUROSCI.5580-10.2011.

Bompas, A., Sumner, P., Muthumumaraswamy, S.D., Singh, K.D., Gilchrist, I.D., 2015. The contribution of pre-stimulus neural oscillatory activity to spontaneous response time variability. Neuroimage 107, 34–45. doi:10.1016/j.neuroimage.2014.11.057.

Busch, N.A., Dubois, J., VanRullen, R., 2009. The phase of ongoing EEG oscillations predicts visual perception. J. Neurosci. 29 (24), 7869–7876. doi:10.1523/JNEUROSCI.0113-09.2009.

Caplan, J.B., Madsen, J.R., Raghavachari, S., Kahana, M.J., 2001 Jul. Distinct patterns of brain oscillations underlie two basic parameters of human maze learning. J Neurophysiol 86 (1), 368–380. doi:10.1152/jn.2001.86.1.368, PMID:11431517 .

Chapeton, J.I., Haque, R., Wittig, J.H., Inati, S.K., Zaghloul, K.A., 2019. Large-scale communication in the human brain is rhythmically modulated through alpha coherence. Curr. Biol. 29 (17), 2801–2811. doi:10.1016/j.cub.2019.07.014, e5.

Chaumon, M., Busch, N.A., 2014. Prestimulus neural oscillations inhibit visual perception via modulation of response gain. J. Cogn. Neurosci. 26 (11), 2514–2529. doi:10.1162/jocn_a_00653.

Cohen, M.R., Maunsell, J.H.R., 2009. Attention improves performance primarily by reducing interneuronal correlations. Nat. Neurosci. 12 (12), 1594–1600. doi:10.1038/nn.2439.

Craddock, M., Poliakoff, E., El-deredy, W., Klepousniotou, E., Lloyd, D.M., 2017. Pre-stimulus alpha oscillations over somatosensory cortex predict tactile misperceptions. Neuropsychologia 96, 9–18. doi:10.1016/j.neuropsychologia.2016.12.030.

Crone, N.E., Miglioretti, D.L., Gordon, B., Lesser, R.P., 1998. Functional mapping of human sensorimotor cortex with electrocorticographic spectral analysis. II. Event-related synchronization in the gamma band. Brain 121 (Pt 12), 2301–2315. doi:10.1093/brain/121.12.2301.

de Pesters, A., Coon, W.G., Brunner, P., Gunduz, A., Ritaccio, A.L., Brunet, N.M., de Weerd, P., Roberts, M.J., Oostenveld, R., Fries, P., Schalk, G., 2016. Alpha power indexes task-related networks on large and small scales: a multimodal ECoG study in humans and a non-human primate. Neuroimage 134, 122–131. doi:10.1016/j.neuroimage.2016.03.074.

Del Percio, C., Marzano, N., Tilgher, S., Fiore, A., Di Ciolo, E., Aschieri, P., Lino, A., Toràn, G., Babiloni, C., Eusebi, F., 2007. Pre-stimulus alpha rhythms are correlated with post-stimulus sensorimotor performance in athletes and non-athletes: a high-resolution EEG study. Clin. Neurophysiol. 118 (8), 1711–1720. doi:10.1016/j.clinph.2007.04.029.

Desikan, R.S., Ségonne, F., Fischl, B., Quinn, B.T., Dickerson, B.C., Blacker, D., Buckner, R.L., Dale, A.M., Maguire, R.P., Hyman, B.T., Albert, M.S., Killiany, R.J., 2006. An automated labeling system for subdividing the human cerebral cortex on MRI scans into gyral based regions of interest. Neuroimage 31 (3), 968–980. doi:10.1016/j.neuroimage.2006.01.021.

Diepen, R.M.van, Mazaheri, A., 2017. Cross-sensory modulation of alpha oscillatory activity: suppression, idling, and default resource allocation. Eur. J. Neurosci. 45 (11), 1431–1438. doi:10.1111/ejn.13570.

Dockree, P.M., Kelly, S.P., Foxe, J.J., Reilly, R.B., Robertson, I.H., 2007. Optimal sustained attention is linked to the spectral content of background EEG activity: greater ongoing tonic alpha (approximately 10Hz) power supports successful phasic goal activation. Eur. J. Neurosci. 25 (3), 900–907. doi:10.1111/j.1460-9568.2007.05324.x.

Donoghue, T., Haller, M., Peterson, E.J., Varma, P., Sebastian, P., Gao, R., Noto, T., Lara, A.H., Wallis, J.D., Knight, R.T., Shestyuk, A., Voytek, B., 2020. Parameterizing neural power spectra into periodic and aperiodic components. Nat. Neurosci. 23 (12), 1655–1665. doi:10.1038/s41593-020-00744-x.

Dougherty, K., Cox, M.A., Ninomiya, T., Leopold, D.A., Maier, A., 2017. Ongoing alpha activity in v1 regulates visually driven spiking responses. Cereb. Cortex 27 (2), 1113–1124. doi:10.1093/cercor/bhv304.

Ergenoglu, T., Demiralp, T., Bayraktaroglu, Z., Ergen, M., Beydagi, H., Uresin, Y., 2004. Alpha rhythm of the EEG modulates visual detection performance in humans. Brain Res. Cogn. Brain Res. 20 (3), 376–383. doi:10.1016/j.cogbrainres.2004.03.009.

Fisch, L., Privman, E., Ramot, M., Harel, M., Nir, Y., Kipervasser, S., Andelman, F., Neufeld, M.Y., Kramer, U., Fried, I., Malach, R., 2009. Neural "ignition": enhanced activation linked to perceptual awareness in human ventral stream visual cortex. Neuron 64 (4), 562–574. doi:10.1016/j.neuron.2009.11.001.

Fischl, B., van der Kouwe, A., Destrieux, C., Halgren, E., Ségonne, F., Salat, D.H., Busa, E., Seidman, L.J., Goldstein, J., Kennedy, D., Caviness, V., Makris, N., Rosen, B., Dale, A.M., 2004. Automatically parcellating the human cerebral cortex. Cereb. Cortex 14 (1), 11–22. doi:10.1093/cercor/bhg087.

Fontolan, L., Morillon, B., Liegeois-Chauvel, C., Giraud, A.-L., 2014. The contribution of frequency-specific activity to hierarchical information processing in the human auditory cortex. Nat. Commun. 5 (1), 4694. doi:10.1038/ncomms5694.

Fries, P., Reynolds, J.H., Rorie, A.E., Desimone, R., 2001. Modulation of oscillatory neuronal synchronization by selective visual attention. Science 291 (5508), 1560–1563. doi:10.1126/science.1055465.

Goldman, R.I., Stern, J.M., Engel, J., Cohen, M.S., 2002. Simultaneous EEG and fMRI of the alpha rhythm. Neuroreport 13 (18), 2487–2492. doi:10.1097/01.wnr.0000047685.08940.d0.

Goris, R.L.T., Movshon, J.A., Simoncelli, E.P., 2014. Partitioning neuronal variability. Nat. Neurosci. 17 (6), 858–865. doi:10.1038/nn.3711.

Grabot, L., Kayser, C., 2020. Alpha activity reflects the magnitude of an individual bias in human perception. J. Neurosci. doi:10.1523/JNEUROSCI.2359-19.2020.

Griffiths, B.J., Mayhew, S.D., Mullinger, K.J., Jorge, J., Charest, I., Wimber, M., Hanslmayr, S., 2019. Alpha/beta power decreases track the fidelity of stimulus-specific information. Elife 8, e49562. doi:10.7554/eLife.49562.

Gundlach, C., Moratti, S., Forschack, N., Müller, M.M., 2020. Spatial Attentional Selection Modulates Early Visual Stimulus Processing Independently of Visual Alpha Modulations. Cereb. Cortex 30 (6), 3686–3703. doi:10.1093/cercor/bhz335.

Gwilliams, L., & King, J.-R. (2020). Recurrent processes support a cascade of hierarchical decisions. ELife, 9, e56603. 10.7554/eLife.56603

Haegens, S., Cousijn, H., Wallis, G., Harrison, P.J., Nobre, A.C., 2014. Inter- and intra-individual variability in alpha peak frequency. Neuroimage 92, 46–55. doi:10.1016/j.neuroimage.2014.01.049.

Haegens, S., Nácher, V., Luna, R., Romo, R., Jensen, O., 2011. $\alpha$-Oscillations in the monkey sensorimotor network influence discrimination performance by rhythmical inhibition of neuronal spiking. Proc. Natl. Acad. Sci. U.S.A. 108 (48), 19377–19382. doi:10.1073/pnas.1117190108.

Haegens, S., Osipova, D., Oostenveld, R., Jensen, O., 2010. Somatosensory working memory performance in humans depends on both engagement and disengagement of regions in a distributed network. Hum. Brain Mapp. 31 (1), 26–35. doi:10.1002/hbm.20842.

Haegens, S., Pathak, Y.J., Smith, E.H., Mikell, C.B., Banks, G.P., Yates, M., Bijanki, K.R., Schevon, C.A., McKhann, G.M., Schroeder, C.E., Sheth, S.A., 2021. Alpha and broadband high-frequency activity track task dynamics and predict performance in controlled decision-making. Psychophysiology e13901. doi:10.1111/psyp.13901.

Hartmann, C., Lazar, A., Nessler, B., Triesch, J., 2015. Where's the noise? Key features of spontaneous activity and neural variability arise through learning in a deterministic network. PLoS Comput. Biol. 11 (12), e1004640. doi:10.1371/journal.pcbi.1004640.

Helfrich, R.F., Schneider, T.R., Rach, S., Trautmann-Lengsfeld, S.A., Engel, A.K., Herrmann, C.S., 2014. Entrainment of brain oscillations by transcranial alternating current stimulation. Curr. Biol. 24 (3), 333–339. doi:10.1016/j.cub.2013.12.041.

Hwang, E.J., Andersen, R.A., 2011. Effects of visual stimulation on LFPs, spikes, and LFP-spike relations in PRR. J. Neurophysiol. 105 (4), 1850–1860. doi:10.1152/jn.00802.2010.

Iemi, L., Busch, N.A., 2018. Moment-to-moment fluctuations in neuronal excitability bias subjective perception rather than strategic decision-making. eNeuro 5 (3). doi:10.1523/ENEURO.0430-17.2018.

Iemi, L., Busch, N.A., Laudini, A., Haegens, S., Samaha, J., Villringer, A., Nikulin, V.V., 2019. Multiple mechanisms link prestimulus neural oscillations to sensory responses. Elife 8, e43620. doi:10.7554/eLife.43620.

Iemi, L., Chaumon, M., Crouzet, S.M., Busch, N.A., 2017. Spontaneous neural oscillations bias perception by modulating baseline excitability. J. Neurosci. 37 (4), 807–819. doi:10.1523/JNEUROSCI.1432-16.2016.

Jasiukaitis, P., Hakerem, G., 1988. The effect of prestimulus alpha activity on the P300. Psychophysiology 25 (2), 157–165. doi:10.1111/j.1469-8986.1988.tb00979.x.

Jensen, O., Mazaheri, A., 2010. Shaping functional architecture by oscillatory alpha activity: gating by inhibition. Front. Hum. Neurosci. 4. doi:10.3389/fnhum.2010.00186.

Jiang, T., Pellizzer, G., Asman, P., Bastos, D., Bhavsar, S., Tummala, S., Prabhu, S., Ince, N.F., 2020. Power modulations of ECoG alpha/beta and gamma bands correlate with time-derivative of force during hand grasp. Front. Neurosci. 14. doi:10.3389/fnins.2020.00100.

Judd, C.M., Kenny, D.A., 1981. Process Analysis: estimating Mediation in Treatment Evaluations. Eval. Rev. 5 (5), 602–619. doi:10.1177/0193841X8100500502.

Kayser, S.J., McNair, S.W., Kayser, C., 2016. Prestimulus influences on auditory perception from sensory representations and decision processes. Proc. Natl. Acad. Sci. 113 (17), 4842–4847. doi:10.1073/pnas.1524087113.

Kelly, S.P., O'Connell, R.G, 2013. Internal and external influences on the rate of sensory evidence accumulation in the human brain. J. Neurosci. 33 (50), 19434–19441. doi:10.1523/JNEUROSCI.3355-13.2013.

King, J.-R., Pescetelli, N., Dehaene, S., 2016. Brain mechanisms underlying the brief maintenance of seen and unseen sensory information. Neuron 92 (5), 1122–1134. doi:10.1016/j.neuron.2016.10.051.

Kirschfeld, K., 2008. Relationship between the amplitude of alpha waves and reaction time. Neuroreport 19 (9), 907–910. doi:10.1097/wnr.0b013e328302c545.

Klimesch, W., Sauseng, P., Hanslmayr, S., 2007. EEG alpha oscillations: the inhibition-timing hypothesis. Brain Res. Rev. 53 (1), 63–88. doi:10.1016/j.brainresrev.2006.06.003.

Kloosterman, N.A., de Gee, J.W., Werkle-Bergner, M., Lindenberger, U., Garrett, D.D., Fahrenfort, J.J., 2019. Humans strategically shift decision bias by flexibly adjusting sensory evidence accumulation. Elife 8, e37321. doi:10.7554/eLife.37321.

Kosciessa, J.Q., Grandy, T.H., Garrett, D.D., Werkle-Bergner, M., 2020. Single-trial characterization of neural rhythms: Potential and challenges. Neuroimage 206, 116331. doi:10.1016/j.neuroimage.2019.116331, Epub 2019 Nov 8. PMID: 31712168.

Lachaux, J.-P., Axmacher, N., Mormann, F., Halgren, E., Crone, N.E., 2012. High-frequency neural activity and human cognition: past, present and possible future of intracranial EEG research. Prog. Neurobiol. 98 (3), 279–301. doi:10.1016/j.pneurobio.2012.06.008.

Lachaux, J.-P., George, N., Tallon-Baudry, C., Martinerie, J., Hugueville, L., Minotti, L., Kahane, P., Renault, B., 2005. The many faces of the gamma band response to complex visual stimuli. Neuroimage 25 (2), 491–501. doi:10.1016/j.neuroimage.2004.11.052.

Lange, J., Oostenveld, R., Fries, P., 2013. Reduced occipital alpha power indexes enhanced excitability rather than improved visual perception. J. Neurosci. 33 (7), 3212–3220. doi:10.1523/JNEUROSCI.3755-12.2013.

Leszczyński, M., Barczak, A., Kajikawa, Y., Ulbert, I., Falchier, A.Y., Tal, I., Haegens, S., Melloni, L., Knight, R.T., Schroeder, C.E., 2020. Dissociation of broadband high-frequency activity and neuronal firing in the neocortex. Sci. Adv. 6 (33), eabb0977. doi:10.1126/sciadv.abb0977.

Limbach, K., Corballis, P.M., 2016. Prestimulus alpha power influences response criterion in a detection task. Psychophysiology 53 (8), 1154–1164. doi:10.1111/psyp.12666.

Linkenkaer-Hansen, K., Nikulin, V.V., Palva, S., Ilmoniemi, R.J., Palva, J.M., 2004. Prestimulus oscillations enhance psychophysical performance in humans. J. Neurosci. 24 (45), 10186–10190. doi:10.1523/JNEUROSCI.2584-04.2004.

Lou, B., Li, Y., Philiastides, M.G., Sajda, P., 2014. Prestimulus alpha power predicts fidelity of sensory encoding in perceptual decision making. Neuroimage 87, 242–251. doi:10.1016/j.neuroimage.2013.10.041.

Lundqvist, M., Bastos, A.M., Miller, E.K., 2020. Preservation and changes in oscillatory dynamics across the cortical hierarchy. J. Cogn. Neurosci. 32 (10), 2024–2035. doi:10.1162/jocn_a_01600.

MacKinnon, D.P., Fairchild, A.J., Fritz, M.S., 2007. Mediation analysis. Annu. Rev. Psychol. 58, 593. doi:10.1146/annurev.psych.58.110405.085542.

MacKinnon, D.P., Krull, J.L., Lockwood, C.M., 2000. Equivalence of the mediation, confounding and suppression effect. Prevent. Sci. 1 (4), 173.

Manning, J.R., Jacobs, J., Fried, I., Kahana, M.J., 2009. Broadband shifts in local field potential power spectra are correlated with single-neuron spiking in humans. J. Neurosci. 29 (43), 13613–13620. doi:10.1523/JNEUROSCI.2041-09.2009.

Maris, E., Oostenveld, R., 2007. Nonparametric statistical testing of EEG- and MEG-data. J. Neurosci. Methods 164 (1), 177–190. doi:10.1016/j.jneumeth.2007.03.024.

Martin, A.B., Yang, X., Saalmann, Y.B., Wang, L., Shestyuk, A., Lin, J.J., Parvizi, J., Knight, R.T., Kastner, S., 2019. Temporal dynamics and response modulation across the human visual system in a spatial attention task: an ECoG study. J. Neurosci. 39 (2), 333–352. doi:10.1523/JNEUROSCI.1889-18.2018.

Mathewson, K.E., Gratton, G., Fabiani, M., Beck, D.M., Ro, T., 2009. To see or not to see: prestimulus alpha phase predicts visual awareness. J. Neurosci. 29 (9), 2725–2732. doi:10.1523/JNEUROSCI.3963-08.2009.

Mathewson, K.E., Lleras, A., Beck, D.M., Fabiani, M., Ro, T., Gratton, G., 2011. Pulsed out of awareness: EEG alpha oscillations represent a pulsed-inhibition of ongoing cortical processing. Front Psychol 2. doi:10.3389/fpsyg.2011.00099.

Mayer, A., Schwiedrzik, C.M., Wibral, M., Singer, W., Melloni, L., 2016. Expecting to see a letter: alpha oscillations as carriers of top-down sensory predictions. Cereb. Cortex 26 (7), 3146–3160. doi:10.1093/cercor/bhv146.

Mayhew, S.D., Ostwald, D., Porcaro, C., Bagshaw, A.P., 2013. Spontaneous EEG alpha oscillation interacts with positive and negative BOLD responses in the visual-auditory cortices and default-mode network. Neuroimage 76, 362–372. doi:10.1016/j.neuroimage.2013.02.070.

Mazaheri, A., Jensen, O., 2008. Asymmetric Amplitude Modulations of Brain Oscillations Generate Slow Evoked Responses. J. Neurosci. 28 (31), 7781–7787. doi:10.1523/JNEUROSCI.1631-08.2008.

Mazaheri, A., Jensen, O., 2010. Rhythmic pulsing: linking ongoing brain activity with evoked responses. Front Hum Neurosci 4, 177. doi:10.3389/fnhum.2010.00177.

Mazaheri, A., van Schouwenburg, M.R., Dimitrijevic, A., Denys, D., Cools, R., Jensen, O., 2014. Region-specific modulations in oscillatory alpha activity serve to facilitate processing in the visual and auditory modalities. Neuroimage 87, 356–362. doi:10.1016/j.neuroimage.2013.10.052.

McNair, S.W., Kayser, S.J., Kayser, C., 2019. Consistent pre-stimulus influences on auditory perception across the lifespan. Neuroimage 186, 22–32. doi:10.1016/j.neuroimage.2018.10.085.

Mehrpour, V., Martinez-Trujillo, J.C., Treue, S., 2020. Attention amplifies neural representations of changes in sensory input at the expense of perceptual accuracy. Nat. Commun. 11 (1), 2128. doi:10.1038/s41467-020-15989-0.

Miller, K.J., Honey, C.J., Hermes, D., Rao, R.P., denNijs, M., Ojemann, J.G., 2014. Broadband changes in the cortical surface potential track activation of functionally diverse neuronal populations. Neuroimage 85 (0 2), 711–720. doi:10.1016/j.neuroimage.2013.08.070.

Miller, K.J., Leuthardt, E.C., Schalk, G., Rao, R.P.N., Anderson, N.R., Moran, D.W., Miller, J.W., Ojemann, J.G., 2007. Spectral Changes in Cortical Surface Potentials during Motor Movement. J. Neurosci. 27 (9), 2424–2432. doi:10.1523/JNEUROSCI.3886-06.2007.

Min, B.-K., Herrmann, C.S., 2007. Prestimulus EEG alpha activity reflects prestimulus top-down processing. Neurosci. Lett. 422 (2), 131–135. doi:10.1016/j.neulet.2007.06.013.

Mitchell, J.F., Sundberg, K.A., Reynolds, J.H., 2009. Spatial Attention Decorrelates Intrinsic Activity Fluctuations in Macaque Area V4. Neuron 63 (6), 879–888. doi:10.1016/j.neuron.2009.09.013.

Mo, J., Schroeder, C.E., Ding, M., 2011. Attentional Modulation of Alpha Oscillations in Macaque Inferotemporal Cortex. J. Neurosci. 31 (3), 878–882. doi:10.1523/JNEUROSCI.5295-10.2011.

Nikulin, V.V., Brismar, T., 2006. Phase synchronization between alpha and beta oscillations in the human electroencephalogram. Neuroscience 137 (2), 647–657. doi:10.1016/j.neuroscience.2005.10.031, Epub 2005 Dec 9. PMID:16338092 .

Nikulin, V.V., Linkenkaer-Hansen, K., Nolte, G., Curio, G., 2010. Non-zero mean and asymmetry of neuronal oscillations have different implications for evoked responses. Clin. Neurophysiol. 121 (2), 186–193. doi:10.1016/j.clinph.2009.09.028.

Nikulin, V.V., Linkenkaer-Hansen, K., Nolte, G., Lemm, S., Müller, K.R., Ilmoniemi, R.J., Curio, G., 2007. A novel mechanism for evoked responses in the human brain. Eur. J. Neurosci. 25 (10), 3146–3154. doi:10.1111/j.1460-9568.2007.05553.x.

Nir, Y., Andrillon, T., Marmelshtein, A., Suthana, N., Cirelli, C., Tononi, G., Fried, I., 2017. Selective neuronal lapses precede human cognitive lapses following sleep deprivation. Nat. Med. 23 (12), 1474–1480. doi:10.1038/nm.4433.

Nir, Y., Fisch, L., Mukamel, R., Gelbard-Sagiv, H., Arieli, A., Fried, I., Malach, R., 2007. Coupling between neuronal firing rate, gamma LFP, and BOLD fMRi is related to interneuronal correlations. Curr. Biol. 17 (15), 1275–1285. doi:10.1016/j.cub.2007.06.066.

Paoletti, D., Braun, C., Vargo, E.J., Zoest, W.van., 2019. Spontaneous pre-stimulus oscillatory activity shapes the way we look: a concurrent imaging and eye-movement study. Eur. J. Neurosci. 49 (1), 137–149. doi:10.1111/ejn.14285.

Pedregosa, F., Varoquaux, G., Gramfort, A., Michel, V., Thirion, B., Grisel, O., Blondel, M., Prettenhofer, P., Weiss, R., Dubourg, V., Vanderplas, J., Passos, A., Cournapeau, D., 2011. Scikit-learn: machine learning in python. In: Machine Learning in Python, pp. 2825–2830.

Peterson, E.J., Rosen, B.Q., Campbell, A.M., Belger, A., Voytek, B., 2018. 1/f neural noise is a better predictor of schizophrenia than neural oscillations. BioRxiv, 113449 doi:10.1101/113449.

Podvalny, E., Noy, N., Harel, M., Bickel, S., Chechik, G., Schroeder, C.E., Mehta, A.D., Tsodyks, M., Malach, R., 2015. A unifying principle underlying the extracellular field potential spectral responses in the human cortex. J. Neurophysiol. 114 (1), 505–519. doi:10.1152/jn.00943.2014.

Potes, C., Brunner, P., Gunduz, A., Knight, R.T., Schalk, G., 2014. Spatial and temporal relationships of electrocorticographic alpha and gamma activity during auditory processing. Neuroimage 97, 188–195. doi:10.1016/j.neuroimage.2014.04.045.

Proskovec, A.L., Wiesman, A.I., Wilson, T.W., 2019. The strength of alpha and gamma oscillations predicts behavioral switch costs. Neuroimage 188, 274–281. doi:10.1016/j.neuroimage.2018.12.016.

Rahn, E., Başar, E., 1993. Enhancement of visual evoked potentials by stimulation during low prestimulus EEG stages. Int. J. Neurosci. 72 (1–2), 123–136. doi:10.3109/00207459308991629.

Rahnev, D., Denison, R.N., 2018. Suboptimality in perceptual decision making. In: The Behavioral and Brain Sciences, pp. 1–107. doi:10.1017/S0140525X18000936.

Ray, S., Crone, N.E., Niebur, E., Franaszczuk, P.J., Hsiao, S.S., 2008. Neural correlates of high-gamma oscillations (60–200hz) in macaque local field potentials and their potential implications in electrocorticography. J. Neurosci. 28 (45), 11526–11536. doi:10.1523/JNEUROSCI.2848-08.2008.

Ray, S., Maunsell, J.H.R., 2011. Different origins of gamma rhythm and high-gamma activity in macaque visual cortex. PLoS Biol. 9 (4), e1000610. doi:10.1371/journal.pbio.1000610.

Rich, E.L., Wallis, J.D., 2017. Spatiotemporal dynamics of information encoding revealed in orbitofrontal high-gamma. Nat. Commun. 8 (1), 1139. doi:10.1038/s41467-017-01253-5.

Rickert, J., Oliveira, S.C.de, Vaadia, E., Aertsen, A., Rotter, S., Mehring, C., 2005. Encoding of movement direction in different frequency ranges of motor cortical local field potentials. J. Neurosci. 25 (39), 8815–8824. doi:10.1523/JNEUROSCI.0816-05.2005.

Roberts, D.M., Fedota, J.R., Buzzell, G.A., Parasuraman, R., McDonald, C.G., 2014. Prestimulus oscillations in the alpha band of the EEG are modulated by the difficulty of feature discrimination and predict activation of a sensory discrimination process. J. Cogn. Neurosci. 26 (8), 1615–1628. doi:10.1162/jocn_a_00569.

Rodriguez, R., Kallenbach, U., Singer, W., Munk, M.H.J., 2004. Short- and long-term effects of cholinergic modulation on gamma oscillations and response synchronization in the visual cortex. J. Neurosci. 24 (46), 10369–10378. doi:10.1523/JNEUROSCI.1839-04.2004.

Rohenkohl, G., Nobre, A.C., 2011. Alpha oscillations related to anticipatory attention follow temporal expectations. J. Neurosci. 31 (40), 14076–14084. doi:10.1523/JNEUROSCI.3387-11.2011.

Romei, V., Brodbeck, V., Michel, C., Amedi, A., Pascual-Leone, A., Thut, G., 2008a. Spontaneous fluctuations in posterior alpha-band EEG activity reflect variability in excitability of human visual areas. Cereb. Cortex 18 (9), 2010–2018. doi:10.1093/cercor/bhm229.

Romei, V., Brodbeck, V., Michel, C., Amedi, A., Pascual-Leone, A., Thut, G., 2008b. Spontaneous fluctuations in posterior $\alpha$-band EEG activity reflect variability in excitability of human visual areas. Cereb. Cortex 18 (9), 2010–2018. doi:10.1093/cercor/bhm229.

Romei, V., Gross, J., Thut, G., 2010. On the role of prestimulus alpha rhythms over occipito-parietal areas in visual input regulation: correlation or causation? J. Neurosci. 30 (25), 8692–8697. doi:10.1523/JNEUROSCI.0160-10.2010.

Salti, M., Monto, S., Charles, L., King, J.-R., Parkkonen, L., Dehaene, S., 2015. Distinct cortical codes and temporal dynamics for conscious and unconscious percepts. Elife 4, e05652. doi:10.7554/eLife.05652.

Samaha, J., Gosseries, O., Postle, B.R., 2017a. Distinct Oscillatory Frequencies Underlie Excitability of Human Occipital and Parietal Cortex. J. Neurosci. 37 (11), 2824–2833. doi:10.1523/JNEUROSCI.3413-16.2017.

Samaha, J., Iemi, L., Haegens, S., Busch, N.A., 2020a. Spontaneous Brain Oscillations and Perceptual Decision-Making. Trends Cogn. Sci. (Regul. Ed.) 24 (8), 639–653. doi:10.1016/j.tics.2020.05.004.

Samaha, J., Iemi, L., Postle, B.R., 2017b. Prestimulus alpha-band power biases visual discrimination confidence, but not accuracy. Conscious. Cogn. 54, 47–55. doi:10.1016/j.concog.2017.02.005.

Samaha, J., LaRocque, J.J., Postle, B.R., 2020b. Spontaneous alpha-band amplitude predicts subjective visibility but not discrimination accuracy during high-level perception. BioRxiv doi:10.1101/2020.07.13.201178, 2020.07.13.201178.

Schaworonkow, N., Blythe, D.A.J., Kegeles, J., Curio, G., Nikulin, V.V., 2015. Power-law dynamics in neuronal and behavioral data introduce spurious correlations. Hum. Brain Mapp. 36 (8), 2901–2914. doi:10.1002/hbm.22816.

Scheeringa, R., Mazaheri, A., Bojak, I., Norris, D.G., Kleinschmidt, A., 2011. Modulation of visually evoked cortical fmri responses by phase of ongoing occipital alpha oscillations. J. Neurosci. 31 (10), 3813–3820. doi:10.1523/JNEUROSCI.4697-10.2011.

Simon, D.M., Wallace, M.T., 2016. Dysfunction of sensory oscillations in Autism Spectrum Disorder. Neurosci. Biobehav. Rev. 68, 848–861. doi:10.1016/j.neubiorev.2016.07.016.

Spaak, E., Bonnefond, M., Maier, A., Leopold, D.A., Jensen, O., 2012. Layer-specific entrainment of gamma-band neural activity by the alpha rhythm in monkey visual cortex. Curr. Biol. 22 (24), 2313–2318. doi:10.1016/j.cub.2012.10.020.

Stephani, T., Waterstraat, G., Haufe, S., Curio, G., Villringer, A., Nikulin, V.V., 2020. Temporal signatures of criticality in human cortical excitability as probed by early somatosensory responses. J. Neurosci. doi:10.1523/JNEUROSCI.0241-20.2020.

Stoller, A., 1949. Slowing of the alpha-rhythm of the electroencephalogram and its association with mental deterioration and epilepsy. J Ment Sci 95 (401), 972–984. doi:10.1192/bjp.95.401.972.

Suzuki, M., Larkum, M., 2017. Dendritic calcium spikes are clearly detectable at the cortical surface. Nat. Commun. 8. doi:10.1038/s41467-017-00282-4.

Tolhurst, D.J., Movshon, J.A., Thompson, I.D., 1981. The dependence of response amplitude and variance of cat visual cortical neurones on stimulus contrast. Exp. Brain Res. 41 (3), 414–419. doi:10.1007/BF00238900.

Tomko, G.J., Crapper, D.R., 1974. Neuronal variability: non-stationary responses to identical visual stimuli. Brain Res. 79 (3), 405–418. doi:10.1016/0006-8993(74)90438-7.

Tran, T.T., Rolle, C.E., Gazzaley, A., Voytek, B., 2020. Linked sources of neural noise contribute to age-related cognitive decline. J. Cogn. Neurosci. 32 (9), 1813–1822. doi:10.1162/jocn_a_01584.

Treue, S., Maunsell, J.H.R., 1996. Attentional modulation of visual motion processing in cortical areas MT and MST. Nature 382 (6591), 539–541. doi:10.1038/382539a0.

Uhlhaas, P.J., Singer, W., 2010. Abnormal neural oscillations and synchrony in schizophrenia. Nat. Rev. Neurosci. 11 (2), 100–113. doi:10.1038/nrn2774.

van den Berg, B., Appelbaum, L.G., Clark, K., Lorist, M.M., Woldorff, M.G., 2016. Visual search performance is predicted by both prestimulus and poststimulus electrical brain activity. Sci. Rep. 6 (1), 37718. doi:10.1038/srep37718.

van Albada, S.J., Robinson, P.A., 2013. Relationships between Electroencephalographic Spectral Peaks Across Frequency Bands. Front Hum Neurosci 7, 56. doi:10.3389/fnhum.2013.00056, PMID:23483663PMCID: PMC3586764.

van Diepen, R.M., Cohen, M.X., Denys, D., Mazaheri, A., 2015. Attention and temporal expectations modulate power, not phase, of ongoing alpha oscillations. J. Cogn. Neurosci. 27 (8), 1573–1586. doi:10.1162/jocn_a_00803.

Van Diepen, R.M., Foxe, J.J., Mazaheri, A., 2019. The functional role of alpha-band activity in attentional processing: the current zeitgeist and future outlook. Curr Opin Psychol 29, 229–238. doi:10.1016/j.copsyc.2019.03.015.

van Dijk, H., Schoffelen, J.-.M., Oostenveld, R., Jensen, O., 2008. Prestimulus oscillatory activity in the alpha band predicts visual discrimination ability. J. Neurosci. 28 (8), 1816–1823. doi:10.1523/JNEUROSCI.1853-07.2008.

van Dijk, H., van der Werf, J., Mazaheri, A., Medendorp, W.P., Jensen, O., 2010. Modulations in oscillatory activity with amplitude asymmetry can produce cognitively relevant event-related responses. Proc. Natl. Acad. Sci. U.S.A. 107 (2), 900–905. doi:10.1073/pnas.0908821107.

van Ede, F., Chekroud, S.R., Stokes, M.G., Nobre, A.C., 2018. Decoding the influence of anticipatory states on visual perception in the presence of temporal distractors. Nat. Commun. 9 (1), 1449. doi:10.1038/s41467-018-03960-z.

van Ede, F., Szebényi, S., Maris, E., 2014. Attentional modulations of somatosensory alpha, beta and gamma oscillations dissociate between anticipation and stimulus processing. Neuroimage 97, 134–141. doi:10.1016/j.neuroimage.2014.04.047.

van Kerkoerle, T., Self, M.W., Dagnino, B., Gariel-Mathis, M.-.A., Poort, J., van der Togt, C., Roelfsema, P.R., 2014. Alpha and gamma oscillations characterize feedback and feedforward processing in monkey visual cortex. Proc. Natl. Acad. Sci. U.S.A. 111 (40), 14332–14341. doi:10.1073/pnas.1402773111.

Voytek, B., Kramer, M.A., Case, J., Lepage, K.Q., Tempesta, Z.R., Knight, R.T., Gazzaley, A., 2015. Age-Related Changes in 1/f Neural Electrophysiological Noise. J. Neurosci. 35 (38), 13257–13265. doi:10.1523/JNEUROSCI.2332-14.2015.

Vugt, B.van, Dagnino, B., Vartak, D., Safaai, H., Panzeri, S., Dehaene, S., Roelfsema, P.R., 2018. The threshold for conscious report: signal loss and response bias in visual and frontal cortex. Science 360 (6388), 537–542. doi:10.1126/science.aar7186.

Walz, J.M., Goldman, R.I., Carapezza, M., Muraskin, J., Brown, T.R., Sajda, P., 2015. Prestimulus EEG Alpha oscillations modulate task-related fMRI BOLD responses to auditory stimuli. Neuroimage 113, 153–163. doi:10.1016/j.neuroimage.2015.03.028.

Watson, B.O., Ding, M., Buzsáki, G., 2018. Temporal coupling of field potentials and action potentials in the neocortex. Eur. J. Neurosci. 48 (7), 2482–2497. doi:10.1111/ejn.13807.

Whitten, T.A., Hughes, A.M., Dickson, C.T., Caplan, J.B., 2011. A better oscillation detection method robustly extracts EEG rhythms across brain state changes: the human alpha rhythm as a test case. Neuroimage 54 (2), 860–874. doi:10.1016/j.neuroimage.2010.08.064, Epub 2010 Aug 31. PMID:20807577 .

Whittingstall, K., Logothetis, N.K., 2009. Frequency-Band Coupling in Surface EEG Reflects Spiking Activity in Monkey Visual Cortex. Neuron 64 (2), 281–289. doi:10.1016/j.neuron.2009.08.016.

Wöstmann, M., Waschke, L., Obleser, J., 2019. Prestimulus neural alpha power predicts confidence in discriminating identical auditory stimuli. Eur. J. Neurosci. 49 (1), 94–105. doi:10.1111/ejn.14226.

Wyart, V., Koechlin, E., 2016. Choice variability and suboptimality in uncertain environments. Curr Opin Behav Sci 11, 109–115. doi:10.1016/j.cobeha.2016.07.003.

Wyart, V., Tallon-Baudry, C., 2009. How ongoing fluctuations in human visual cortex predict perceptual awareness: baseline shift versus decision bias. J. Neurosci. 29 (27), 8715–8725. doi:10.1523/JNEUROSCI.0962-09.2009.

Yang, A.I., Wang, X., Doyle, W.K., Halgren, E., Carlson, C., Belcher, T.L., Cash, S.S., Devinsky, O., Thesen, T., 2012. Localization of dense intracranial electrode arrays using magnetic resonance imaging. Neuroimage 63 (1), 157–165. doi:10.1016/j.neuroimage.2012.06.039.

Zhang, Y., Wang, X., Bressler, S.L., Chen, Y., Ding, M., 2008. Prestimulus cortical activity is correlated with speed of visuomotor processing. J. Cogn. Neurosci. 20 (10), 1915–1925. doi:10.1162/jocn.2008.20132.